

Embedded minimal surfaces of finite topology

William H. Meeks III^{*} Joaquín Pérez[†]

March 5, 2022

Abstract

In this paper we prove that a complete, embedded minimal surface M in \mathbb{R}^3 with finite topology and compact boundary (possibly empty) is conformally a compact Riemann surface \bar{M} with boundary punctured in a finite number of interior points and that M can be represented in terms of meromorphic data on its conformal completion \bar{M} . In particular, we demonstrate that M is a minimal surface of finite type and describe how this property permits a classification of the asymptotic behavior of M .

Mathematics Subject Classification: Primary 53A10, Secondary 49Q05, 53C42

Key words and phrases: Minimal surface, helicoid with handles, infinite total curvature, flux vector, minimal surface of finite type, asymptotic behavior.

1 Introduction.

Based on work of Colding and Minicozzi [7], Meeks and Rosenberg [19] proved that a properly embedded, simply connected minimal surface in \mathbb{R}^3 is a plane or a helicoid. In the last page of their paper, they described how their proof of the uniqueness of the helicoid could be modified to prove:

Any nonplanar, properly embedded minimal surface M in \mathbb{R}^3 with one end, finite topology and infinite total curvature satisfies the following properties:

1. *M is conformally a compact Riemann surface \bar{M} punctured at a single point.*
2. *M is asymptotic to a helicoid.*
3. *M can be expressed analytically in terms of meromorphic data on \bar{M} .*

A rigorous proof of the above statement has been given by Bernstein and Breiner [1].

In our survey [13] and book [14], we outlined the proof by Meeks and Rosenberg of the uniqueness of the helicoid and at the end of this outline we mentioned how some difficult parts of this proof could be simplified using some results of Colding and Minicozzi in [3], and referred the reader to the present paper for details. Actually, we will consider the more general problem of describing the asymptotic behavior, conformal structure and analytic representation

^{*}This material is based upon work for the NSF under Award No. DMS - 1309236. Any opinions, findings, and conclusions or recommendations expressed in this publication are those of the authors and do not necessarily reflect the views of the NSF.

[†]Research partially supported by the MINECO/FEDER grant no. MTM2011-22547.

of an annular end of any *complete*, injectively immersed¹ minimal surface M in \mathbb{R}^3 with compact boundary and finite topology. Although not explicitly stated in the paper [8] by Colding and Minicozzi, the results contained there imply that such an M is *properly embedded*² in \mathbb{R}^3 ; we will use this properness property of M in the proof of Theorem 1.1 below. We also remark that Meeks, Pérez and Ros [15] have proved the following more general properness result: If M is a complete, injectively immersed minimal surface of finite genus, compact boundary and a countable number of ends in \mathbb{R}^3 , then M is proper (this follows from part 3-B of Theorem 1.3 in [15]). Since properly embedded minimal annuli $E \subset \mathbb{R}^3$ with compact boundary and finite total curvature are conformally punctured disks, are asymptotic to the ends of planes and catenoids and have a well-understood analytic description in terms of meromorphic data on their conformal completion, we will focus our attention on the case that the minimal annulus has infinite total curvature.

Theorem 1.1 *Let $E \subset \mathbb{R}^3$ be a complete, embedded minimal annulus with infinite total curvature and compact boundary. Then, the following properties hold:*

1. *E is properly embedded in \mathbb{R}^3 .*
2. *E is conformally diffeomorphic to a punctured disk.*
3. *After applying a suitable homothety and rigid motion to a subend of E , then:*
 - a. *The holomorphic height differential $dh = dx_3 + id x_3^*$ of E is $dh = (1 + \frac{\lambda}{z-\mu}) dz$, defined on $D(\infty, R) = \{z \in \mathbb{C} \mid |z| \geq R\}$ for some $R > 0$, where $\lambda \geq 0$ and $\mu \in \mathbb{C}$. In particular, dh extends meromorphically across infinity with a double pole.*
 - b. *The stereographic projection $g: D(\infty, R) \rightarrow \mathbb{C} \cup \{\infty\}$ of the Gauss map of E can be expressed as $g(z) = e^{iz+f(z)}$ for some holomorphic function f in $D(\infty, R)$ with $f(\infty) = 0$.*
 - c. *E is asymptotic to the end of a helicoid if and only if it has zero flux (in particular, the number λ in the previous item 3a vanishes in this case).*

Since complete embedded minimal surfaces with finite topology and empty boundary are properly embedded in \mathbb{R}^3 [8], and properly embedded minimal surfaces with more than one end and finite topology have finite total curvature [10], then we have the following immediate corollary (which also appears in [1]). Note also that the zero flux condition in item 3c of Theorem 1.1 holds by Cauchy's theorem when the surface has just one end.

Corollary 1.2 *Suppose that $M \subset \mathbb{R}^3$ is a complete, embedded minimal surface with finite topology and empty boundary. Then, M is conformally a compact Riemann surface \overline{M} punctured in a finite number of points and M can be described analytically in terms of meromorphic data $\frac{dg}{g}, dh$ on \overline{M} , where g and dh denote the stereographically projected Gauss map and the height differential of M , after a suitable rotation in \mathbb{R}^3 . Furthermore, M has bounded Gaussian curvature and each of its ends is asymptotic in the C^k -topology (for any $k \in \mathbb{N}$) to a plane or a half-catenoid (if M has finite total curvature) or to a helicoid (if M has infinite total curvature).*

¹That is, M has no self-intersections and its intrinsic topology may or may not agree with the subspace topology as a subset of \mathbb{R}^3 .

²By this we mean that the intrinsic topology on M coincides with the subspace topology and the intersection of M with every closed ball in \mathbb{R}^3 is compact in M .

In order to state the next result, we need the following notation. Given $R, h > 0$, let

$$C(R) = \{(x_1, x_2, x_3) \mid x_1^2 + x_2^2 \leq R^2\}, \quad (1)$$

$$C(R, h) = C(R) \cap \{|x_3| \leq h\}, \quad (2)$$

$$D(\infty, R) = \{x_3 = 0\} \cap [\mathbb{R}^3 - \text{Int}(C(R))].$$

A *multivalued graph* over $D(\infty, R)$ is the graph $\Sigma = \{(re^{i\theta}, u(r, \theta))\} \subset \mathbb{C} \times \mathbb{R} \equiv \mathbb{R}^3$ of a smooth function $u = u(r, \theta)$ defined on the universal cover $\tilde{D}(\infty, R) = \{(r, \theta) \mid r \geq R, \theta \in \mathbb{R}\}$ of $D(\infty, R)$.

The next descriptive result is a consequence of Theorem 7.1 below, and provides the existence of a collection $\mathcal{E} = \{E_{a,b} \mid a, b \in [0, \infty)\}$ of properly embedded minimal annuli in \mathbb{R}^3 such that any complete, embedded minimal annulus E with compact boundary and infinite total curvature in \mathbb{R}^3 is, after a rigid motion, asymptotic to a homothetic scaling of exactly one of the surfaces in \mathcal{E} . The image in Figure 1 describes how the flux vector

$$(a, 0, -b) = \int_{\partial E_{a,b}} \eta$$

of the minimal annulus $E_{a,b}$ influences its geometry (here η refers to the unit conormal vector exterior to $E_{a,b}$ along its boundary).

Theorem 1.3 (Asymptotics of embedded minimal annular ends) *Given $a, b \geq 0$, there exist $R > 0$ and a properly embedded minimal annulus $E_{a,b} \subset \mathbb{R}^3$ with compact boundary and flux vector $(a, 0, -b)$ along its boundary, such that the following statements hold.*

1. $E_{a,b} - C(R)$ consists of two disjoint multivalued graphs Σ_1, Σ_2 over $D(\infty, R)$ of functions $u_1, u_2: \tilde{D}(\infty, R) \rightarrow \mathbb{R}$ such that their gradients, with respect to the metric on $\tilde{D}(\infty, R)$ obtained by pulling back the standard flat metric in $D(\infty, R)$, satisfy $\nabla u_i(r, \theta) \rightarrow 0$ as $r \rightarrow \infty$, and the separation function $w(r, \theta) = u_1(r, \theta) - u_2(r, \theta)$ between both multivalued graphs converges to π as $r + |\theta| \rightarrow \infty$. Furthermore for θ fixed and $i = 1, 2$,

$$\lim_{r \rightarrow \infty} \frac{u_i(r, \theta)}{\log(\log(r))} = \frac{b}{2\pi}. \quad (3)$$

2. The translated surfaces $E_{a,b} - (0, 0, 2\pi n + \frac{b}{2\pi} \log n)$ (resp. $E_{a,b} + (0, 0, 2\pi n - \frac{b}{2\pi} \log n)$) converge as $n \rightarrow \infty$ to a right-handed vertical helicoid H_T (resp. H_B) with maximum absolute Gaussian curvature 1 along its axis such that

$$H_B = H_T + (0, a/2, 0). \quad (4)$$

Note that equations (3), (4) imply that for different values of a, b , the related surfaces $E_{a,b}$ are not asymptotic after a rigid motion and homothety.

3. The annuli $E_{0,b}$, $b \in \mathbb{R}$, are each invariant under reflection across the x_3 -axis l , and $l \cap E_{0,b}$ contains two infinite rays. Furthermore, $E_{0,0}$ is the end of a vertical helicoid.
4. Up to a rotation and homothety by some $\rho \in \mathbb{R} - \{0\}$, every complete, embedded minimal annulus in \mathbb{R}^3 with compact boundary and infinite total curvature is asymptotic to exactly one of the surfaces $E_{a,b}$.

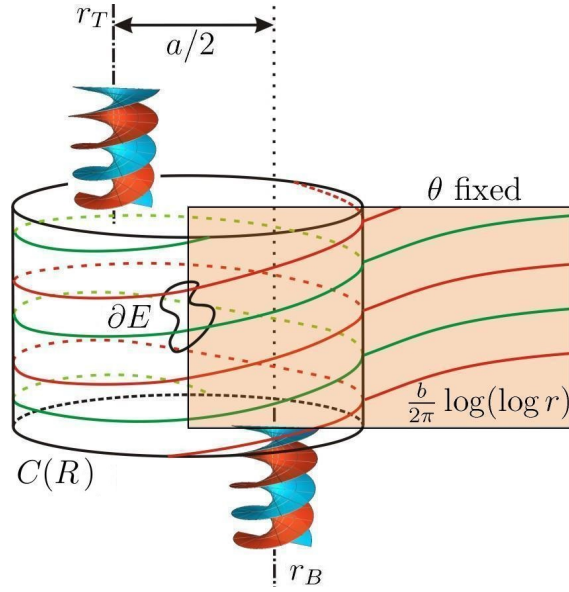


Figure 1: The embedded annulus $E = E_{a,b}$ with flux vector $(a, 0, -b)$ (see Theorem 1.3) has the following description. Outside the infinite vertical cylinder $C(R)$, E consists of two horizontal multivalued graphs with asymptotic spacing π between them. The translated surfaces $E - (0, 0, 2\pi n + \frac{b}{2\pi} \log n)$ (resp. $E + (0, 0, 2\pi n - \frac{b}{2\pi} \log n)$) converge as $n \rightarrow \infty$ to a vertical helicoid H_T (resp. H_B) such that $H_B = H_T + (0, a/2, 0)$ (in the picture, r_T, r_B refer to the axes of H_T, H_B). The intersection of $E - C(R)$ with a vertical half-plane bounded by the x_3 -axis consists of an infinite number of curves, each being a graph of a function $u(r)$ that satisfies the property $\frac{u(r)}{\log(\log r)}$ converges to $\frac{b}{2\pi}$ as the radial distance r to the x_3 -axis tends to ∞ .

As mentioned above, Bernstein and Breiner [1] have given a proof of Corollary 1.2 in the infinite total curvature setting, which is just Theorem 1.1 in the special case that the annulus E is the end of a complete, embedded minimal surface M with finite topology, one end and empty boundary. Our proof of Theorem 1.1 and the proof of Bernstein and Breiner in the above special case, apply arguments that Meeks and Rosenberg [19] used to understand the asymptotic behavior of an E with zero flux, and to show that such an E has finite type³ (even in the case with nonzero flux, this finite type property will follow from application of Corollary 1.2 in our previous paper [12]). Once E is proven to have finite type, then Meeks and Rosenberg, as well as Bernstein and Breiner, appeal to results of Hauswirth, Pérez and Romon [11] on the geometry of embedded, minimal annular ends of finite type to complete the proof. In our proof of Theorem 1.3, we essentially avoid reference to the results in [11] by using self-contained arguments, some of which have a more geometric, less analytic nature than those in [11]. Central to most of these proofs are the results of Colding and Minicozzi [3, 5, 6, 7, 8, 9].

We refer the interested reader to our paper [15] with Ros on the embedded Calabi-Yau problem. More precisely, this paper explains the structure of simple limit ends of complete, injectively immersed minimal surfaces $M \subset \mathbb{R}^3$ of finite genus and compact boundary, which together with Theorems 1.1 and 1.3 in this paper, improve our understanding of the conformal structure, asymptotic behavior and analytic description of the ends of properly embedded minimal surfaces in \mathbb{R}^3 that have compact boundary and finite genus. An outstanding open question related to the embedded Calabi-Yau problem asks whether every complete, injectively immersed minimal surface in \mathbb{R}^3 with finite genus, compact boundary and an infinite number of ends, must have only a countable number of ends, since such minimal surfaces are properly embedded in \mathbb{R}^3 with exactly one or two limit ends; see [15] for further discussion and partial results on this open problem.

2 Weierstrass representation of a minimal surface of finite type.

Recall that the Gauss map of an immersed minimal surface M in \mathbb{R}^3 can be viewed as a meromorphic function $g: M \rightarrow \mathbb{C} \cup \{\infty\}$ on the underlying Riemann surface, after stereographic projection from the north pole of the unit sphere. Furthermore, the harmonicity of the third coordinate function x_3 of M allows us to define (at least locally) its harmonic conjugate function x_3^* ; hence, the *height differential*⁴ $dh = dx_3 + i dx_3^*$ is a holomorphic differential on M . As usual, we will refer to the pair (g, dh) as the *Weierstrass data* of M , and the minimal immersion $X: M \rightarrow \mathbb{R}^3$ can be expressed up to translation by $X(p_0)$, $p_0 \in M$, by

$$X(p) = \operatorname{Re} \int_{p_0}^p \left(\frac{1}{2} \left(\frac{1}{g} - g \right), \frac{i}{2} \left(\frac{1}{g} + g \right), 1 \right) dh. \quad (5)$$

It is well-known (see Osserman [20] for details) that this procedure has a converse, namely if M is a Riemann surface, $g: M \rightarrow \mathbb{C} \cup \{\infty\}$ is a meromorphic function and dh is a holomorphic one-form on M , such that the zeros of dh coincide with the poles and zeros of g with the same

³See Definition 2.1 for the notion of a minimal surface of finite type.

⁴The height differential might not be exact since x_3^* need not be globally well-defined on M . Nevertheless, the notation dh is commonly accepted and we will also make use of it here.

order, and for any closed curve $\gamma \subset M$, the following equalities hold:

$$\overline{\int_{\gamma} g dh} = \int_{\gamma} \frac{dh}{g}, \quad \operatorname{Re} \int_{\gamma} dh = 0, \quad (6)$$

(where \bar{z} denotes the complex conjugate of $z \in \mathbb{C}$), then the map $X: M \rightarrow \mathbb{R}^3$ given by (5) is a conformal minimal immersion with Weierstrass data (g, dh) .

Minimal surfaces M which satisfy the property of having *finite type*, as described in the next definition, can be defined analytically from data obtained by integrating certain meromorphic one-forms on M , which moreover extend meromorphically to the conformal completion of M .

Definition 2.1 (Finite Type) A minimal immersion $X: M \rightarrow \mathbb{R}^3$ is said to have *finite type* if it satisfies the following two properties.

1. The underlying Riemann surface to M is conformally diffeomorphic to a compact Riemann surface \bar{M} with (possibly empty) compact boundary, punctured in a finite nonempty set $\mathcal{E} \subset \operatorname{Int}(\bar{M})$.
2. Given an end $e \in \mathcal{E}$ of M , there exists a rotation of the surface in \mathbb{R}^3 such that if (g, dh) is the Weierstrass data of M after this rotation, then $\frac{dg}{g}$ and dh extend across the puncture e to meromorphic one-forms on a neighborhood of e in \bar{M} .

Therefore, complete immersed minimal surfaces with finite total curvature are of finite type, and the basic example of a surface with finite type but infinite total curvature is the helicoid ($M = \mathbb{C}$, $g(z) = e^{iz}$, $dh = dz$). Finite type minimal surfaces were first studied by Rosenberg [21]; we note that his definition of finite type differs somewhat from our definition above. An in-depth study of *embedded* minimal annular ends of finite type with exact height differentials was made by Hauswirth, Pérez and Romon in [11]. Some of the results in this paper extend the results in [11] to the case where the height differential of the surface might possibly be not exact.

3 The conformal type, height differential and Gauss map of embedded minimal annuli.

Throughout this section, we will fix a complete, injectively immersed minimal surface $M \subset \mathbb{R}^3$ with infinite total curvature, where M is an annulus diffeomorphic to $\mathbb{S}^1 \times [0, \infty)$. By the main result in Colding and Minicozzi [8] (which holds in this setting of compact boundary), M is properly embedded in \mathbb{R}^3 . Our goal in this section is to prove that after a rotation and a replacement of M by a subend, M is conformally diffeomorphic to $D(\infty, 1)$, its height differential extends meromorphically across the puncture ∞ with a double pole, and the meromorphic Gauss map $g: D(\infty, 1) \rightarrow \mathbb{C} \cup \{\infty\}$ of M has the form $g(z) = z^k e^{H(z)}$, where $k \in \mathbb{Z}$ and H is holomorphic in $D(\infty, 1)$.

In Theorem 1.2 of [17], Meeks, Pérez and Ros proved that a complete embedded minimal surface with compact boundary fails to have quadratic decay of curvature⁵ if and only if it does

⁵A properly embedded surface $M \subset \mathbb{R}^3$ has *quadratic decay of curvature* if the function $p \in M \mapsto |K_M|(p)|p|^2$ is bounded, where $|K_M|$ denotes the absolute Gaussian curvature function of M .

not have finite total curvature. Since we are assuming that M has infinite total curvature, then it does not have quadratic decay of curvature.

Let $\{\lambda_n\}_n \subset \mathbb{R}^+$ be a sequence with $\lambda_n \rightarrow 0$ as $n \rightarrow \infty$. We next analyze the structure of the limit of (a subsequence of) the $\lambda_n M$. In our setting with compact boundary we need to be careful at this point, since compactness results as in Colding and Minicozzi [7, 9] cannot be applied directly. In the sequel, $\mathbb{B}(q, R)$ will denote the open ball of radius $R > 0$ centered at $q \in \mathbb{R}^3$, and $\overline{\mathbb{B}}(q, R)$ its closure.

Lemma 3.1 *The sequence $\{\lambda_n M\}_n$ has locally positive injectivity radius in $\mathbb{R}^3 - \{\vec{0}\}$, in the sense that for every $q \in \mathbb{R}^3 - \{\vec{0}\}$, there exists $\varepsilon_q \in (0, |q|)$ and $n_q \in \mathbb{N}$ such that for $n > n_q$, the injectivity radius functions of the surfaces $\lambda_n M$ restricted to $\mathbb{B}(q, \varepsilon_q) \cap (\lambda_n M)$ form a sequence of functions which is uniformly bounded away from zero.*

Proof. Arguing by contradiction, suppose that there exists a point $q \in \mathbb{R}^3 - \{\vec{0}\}$ and points $q_n \in \lambda_n M$ converging to q as $n \rightarrow \infty$, such that the injectivity radius functions of $\lambda_n M$ at q_n converges to zero as $n \rightarrow \infty$. Since the $\lambda_n M$ have nonpositive Gaussian curvature, then (after extracting a subsequence) we can find a sequence of pairwise disjoint embedded geodesic loops $\gamma'_n \subset \mathbb{B}(q, 1/n) \cap (\lambda_n M)$ with at most one cusp at q_n , and with the lengths of these loops tending to zero as n tends to infinity. These curves γ'_n produce related pairwise disjoint embedded geodesic loops γ_n on M with at most one cusp, and the sequence $\{\gamma_n\}_n$ diverges in M . By the Gauss-Bonnet formula, the curves γ_n are homotopically nontrivial and hence topologically parallel to the boundary of M (since M is an annulus). Therefore, the Gauss-Bonnet formula implies that M has finite total curvature, which is a contradiction. This contradiction proves the lemma. \square

Since the surface M does not have quadratic decay of curvature, there exists a divergent sequence of points $\{p_n\}_n \subset M$ (hence p_n also diverges in \mathbb{R}^3) such that $|K_M|(p_n) |p_n|^2 \rightarrow \infty$ as $n \rightarrow \infty$. Consider the sequence of positive numbers $\lambda_n = |p_n|^{-1} \rightarrow 0$. By Lemma 3.1, the sequence $\{\lambda_n M\}_n$ has locally positive injectivity radius in $\mathbb{R}^3 - \{\vec{0}\}$. This property lets us apply Theorem 1.6 of [18] to the sequence of surfaces with boundary $M_n = (\lambda_n M) \cap \overline{\mathbb{B}}(\vec{0}, n) \subset \mathbb{R}^3 - \{\vec{0}\}$ and to the closed countable set $W = \{\vec{0}\}$; since the M_n have genus zero and compact boundary, then item 7.3 of Theorem 1.6 of [18] ensures that after extracting a subsequence, the M_n converge as $n \rightarrow \infty$ to a foliation \mathcal{F} of \mathbb{R}^3 by parallel planes. The convergence of the M_n to \mathcal{F} is C^α , $\alpha \in (0, 1)$, away from a set S that consists of one or two straight lines orthogonal to the planes in \mathcal{F} . The case of two lines in S does not occur by the following reason; if it occurs, then there is a limit parking garage structure with two oppositely oriented columns (see Section 3 of [16] for the notion of parking garage structure), and the surfaces M_n contain closed geodesics γ_n that converge with multiplicity two to a straight line segment that joins orthogonally the two column lines (see item (5.2) in Theorem 1.1 of [16] for a similar statement, whose proof can be adapted to this situation). After passing to a subsequence, the geodesics $\Gamma_n = |p_n| \gamma_n \subset M$ are pairwise disjoint, which is impossible by the Gauss-Bonnet formula applied to the annulus $A(n) \subset M$ bounded by $\Gamma_1 \cup \Gamma_n$, as M has infinite total curvature. Therefore, S consists of a single straight line.

Also note that under these homothetic shrinkings of M , the boundary components ∂_n of M_n corresponding to the homothetically shrunk boundary component of M collapse into the origin $\vec{0}$ as $n \rightarrow \infty$. We claim that the line S passes through $\vec{0}$. To prove this, suppose the claim fails and take $R > 0$ such that S does not intersect the closed ball $\overline{\mathbb{B}}(\vec{0}, 4R)$. Assume

that n is chosen sufficiently large so that $\partial_n \subset \mathbb{B}(\vec{0}, R)$. Recall that we defined in (1) the vertical solid cylinder $C(R)$ of radius $R > 0$ about the x_3 -axis. Since the surfaces M_n are converging away from S to a minimal parking garage structure of \mathbb{R}^3 with associated foliation by horizontal planes, and S does not intersect $\mathbb{B}(\vec{0}, 4R)$, then for n large, the component Δ_n of $M_n \cap C(R, R)$ that contains ∂_n (with the notation in (2)) must be a smooth compact surface with its entire boundary in $\partial C(R)$; furthermore, every component of $\partial \Delta_n$ is a graph over the circle $\partial C(R) \cap \{x_3 = 0\}$ and has total curvature less than 3π . As each M_n is contained in a minimal annulus, then the convex hull property implies that Δ_n is an annulus. Since the total geodesic curvatures of $\partial \Delta_n$ are uniformly bounded, the Gauss-Bonnet formula implies that the total Gaussian curvatures of the compact annuli Δ_n are also uniformly bounded. However, as the surface M has infinite total curvature, then the total Gaussian curvatures of the compact annuli Δ_n are not uniformly bounded. This contradiction proves that the line S passes through $\vec{0}$.

Furthermore, this limit foliation \mathcal{F} can be seen to be independent of the sequence of positive numbers λ_n (this comes from the fact that when one patches together multivalued minimal graphs coming from different scales, then the obtained surface is still a multivalued graph over a fixed plane, see Part II in [4] for more details). Hence, after a rotation of the initial surface M in \mathbb{R}^3 , we may assume that the planes in \mathcal{F} are horizontal. These arguments of patching together multivalued minimal graphs coming from different scales allows us to state the following result.

Lemma 3.2 *There exist positive numbers δ, R_1 and a solid vertical hyperboloid,*

$$\mathcal{H} = \mathcal{H}(\delta, R_1) = \{(x_1, x_2, x_3) \in \mathbb{R}^3 \mid x_1^2 + x_2^2 < \delta^2 x_3^2 + R_1^2\} \quad (7)$$

such that $M - \mathcal{H}$ consists of two multivalued graphs (the projection $(x_1, x_2, x_3) \mapsto (x_1, x_2)$ restricts to a local diffeomorphism onto its image inside the (x_1, x_2) -plane P).

Remark 3.3 *The arguments above use the uniqueness of the helicoid (when applying Theorem 1.6 in [18]). However, for a simply connected surface \widehat{M} without boundary (not an annulus M with compact boundary), both the convergence of $\lambda_n \widehat{M}$ to a foliation of \mathbb{R}^3 by planes and the validity of Lemma 3.2 (after a rotation in \mathbb{R}^3) follow directly from the main results in [7], without reference to the discussion in the previous paragraphs. We make this remark here to warn the reader that we will be applying the next proposition, which depends on Lemma 3.2, in the simplified proof of Theorem 4.1 below on the uniqueness of the helicoid.*

By work of Colding and Minicozzi, any embedded minimal k -valued graph with k sufficiently large contains a 2-valued subgraph which can be approximated by the multivalued graph of a helicoid with an additional logarithmic term. This approximation result, which appears as Corollary 14.3 in Colding and Minicozzi [3], together with estimates for the decay of the separation between consecutive sheets of a multivalued graph (equations (18.1) in [3] or (5.9) in [5], which in turn follow from Proposition 5.5 in [5], and from Proposition II.2.12 and Corollary II.3.7 in [4]), are sufficient to prove that, with the notation in Lemma 3.2, each of the two multivalued graphs G_1, G_2 in $M - \mathcal{H}$ contains multivalued subgraphs G'_1, G'_2 , respectively given by functions $u_1(r, \theta), u_2(r, \theta)$, such that $\frac{\partial u_i}{\partial \theta}(r, \theta) > 0$ for every (r, θ) and $i = 1, 2$ (resp. $\frac{\partial u_i}{\partial \theta}(r, \theta) < 0$ when the multivalued graphs G'_1, G'_2 spiral downward in a counter clockwise manner); furthermore the boundary curves of the subgraphs G'_1, G'_2 can be assumed to lie on the boundary of another hyperboloid $\mathcal{H}' = \mathcal{H}(\delta, R_2)$ for some $R_2 > R_1$. This observation

concerning $\frac{\partial u_i}{\partial \theta}(r, \theta) > 0$ was also made by Bernstein and Breiner using the same arguments, see Proposition 3.3 in [2]. We refer the reader to their paper for details.

With the above discussion in mind, we are ready to describe the main result of this section.

Proposition 3.4 *After a rotation of M so that the foliation \mathcal{F} is horizontal, then:*

1. *There is a subend M' of M such that each horizontal plane $P_t = x_3^{-1}(t)$ in \mathcal{F} intersects M' transversely in either a proper curve at height t or in two proper arcs, each with its single end point on the boundary of M' . More specifically, there exists a compact solid cylinder $C(R, h)$ with $\partial M \subset \text{Int}(C(R, h))$ whose top and bottom disks each intersects M transversely in a compact arc and whose side $\{x_1^2 + x_2^2 = R^2, |x_3| \leq h\}$ intersects M transversely in two compact spiraling arcs $\beta_1(\theta), \beta_2(\theta)$ with $\langle \frac{d\beta_i}{d\theta}, (0, 0, 1) \rangle > 0, i = 1, 2$ (after a possible replacement of M by $-M$), where θ is the multivalued angle parameter over the circle $\partial C(R, h) \cap P_0$, and so that $M' = M - \text{Int}(C(R, h))$ is the desired subend.*
2. *The end M' is conformally diffeomorphic to $D(\infty, 1)$.*
3. *There exists $k \in \mathbb{Z}$ and a holomorphic function H on $D(\infty, 1)$ such that the stereographically projected Gauss map of M' is $g(z) = z^k e^{H(z)}$ on $D(\infty, 1)$. Furthermore, the height differential $dh = dx_3 + i dx_3^*$ of M' extends meromorphically to $D(\infty, 1) \cup \{\infty\}$ with a double pole at ∞ .*

Proof. We first construct the cylinder $C(R, h)$. Choose R and h large enough so that $\partial M \subset \text{Int}(C(R, h))$ and so that the side $C(R, h) \cap \partial C(R)$ intersects the multivalued graphs G'_1, G'_2 , transversely in two compact spiraling arcs $\beta_1(\theta), \beta_2(\theta)$ with $\langle \frac{d\beta_i}{d\theta}, (0, 0, 1) \rangle > 0, i = 1, 2$ (we may assume this sign of $\frac{d\beta_i}{d\theta}$ after replacing M by $-M$). Note that by increasing the radius R and height h , the sets $M \cap C(R, h)$ define a compact exhaustion of M , since M is proper. These R, h are taken so that $R \gg h$ in order to ensure that $C(R, h) \cap \partial C(R)$ is disjoint from the hyperboloid \mathcal{H} defined by (7), and $C(R, h) \cap \partial C(R)$ intersects the multivalued graphs G'_1 , and G'_2 in the above spiraling-type arcs β_1, β_2 . Also take R, h large enough so that the component of $M \cap C(R, h)$ which contains ∂M , also contains β_1, β_2 in its boundary. Without loss of generality, we can assume that the top and bottom disks $D_h \subset P_h, D_{-h} \subset P_{-h}$ of $C(R, h)$ each intersects M transversely. The convex hull property implies that there are no closed curve components in $(D_h \cup D_{-h}) \cap M$, and thus $(D_h \cup D_{-h}) \cap M$ consists of two compact arcs $\alpha_T \subset D_h, \alpha_B \subset D_{-h}$, see Figure 2. Hence, $M' = M - \text{Int}(C(R, h))$ is an annular subend of M . Furthermore, each of the planes P_{-h}, P_h intersects M' in a connected proper curve $\tilde{\alpha}_B, \tilde{\alpha}_T$ that contains α_B, α_T , respectively; this is because each of $\tilde{\alpha}_B, \tilde{\alpha}_T$ intersects each of the cylinders $\partial C(R'), R' \geq R$, at exactly two points. By our choices of G'_1 , and G'_2 , each plane $P_t, t \in (-h, h)$, intersects M' in a pair of proper arcs each with one end point in $\partial M'$. Since each of the planes $P_t, |t| \geq h$, intersects each of G'_1 , and G'_2 transversely in a single proper arc with end point in the boundary of the respective multivalued graph, then elementary Morse theory and the convex hull property imply that each of these planes intersects M' transversely in a single proper curve. Since M' intersects some horizontal plane in a connected proper curve, then the remaining statements in the proposition follow directly from Corollary 1.2 in [12]. \square

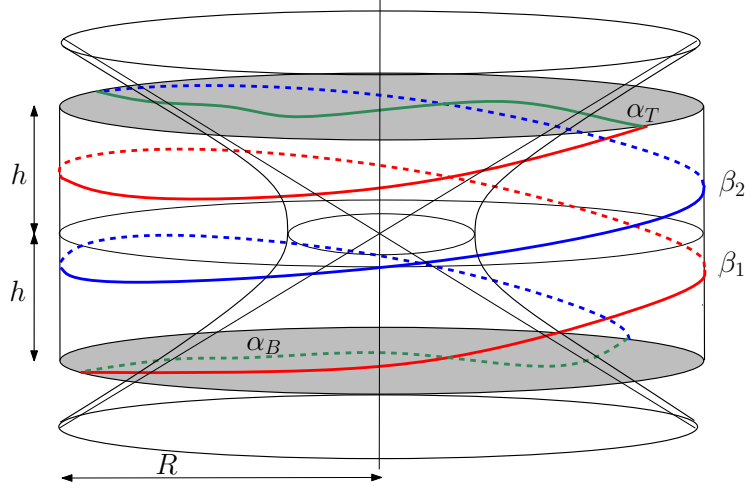


Figure 2: x_3 is monotonic along the curves $\beta_1, \beta_2 = M' \cap [\partial C(R) \cap \{0 < x_3 < h\}]$ (red, blue), and constant along the top and bottom arcs $\alpha_T, \alpha_B = M' \cap [\partial C(R, h) - \{0 < x_3 < h\}]$ (green).

4 Uniqueness of the helicoid.

In this section we will apply Proposition 3.4 to simplify the original proof by Meeks and Rosenberg of the uniqueness of the helicoid among properly embedded, simply connected, nonflat minimal surfaces in \mathbb{R}^3 . The proof we give below only uses the one-sided curvature estimates by Colding and Minicozzi (Theorem 0.2 in [7]), Proposition 3.4 in this paper, and some arguments taken from the end of [19]. Since the uniqueness of the helicoid given in [19] is not used in the proof by Colding and Minicozzi that completeness implies properness for embedded, finite topology minimal surfaces, then we can replace the hypothesis of properness by the weaker one of completeness in the above statement of uniqueness of the helicoid.

Theorem 4.1 *If $M \subset \mathbb{R}^3$ is a complete, embedded, simply connected minimal surface, then M is either a plane or a helicoid.*

Proof. Assume M is not flat. By Proposition 3.4, the conformal type of M is \mathbb{C} and its height differential $dh = dx_3 + idx_3^*$ extends meromorphically to ∞ with a double pole. Therefore $dh = \lambda dz$ for some $\lambda \in \mathbb{C}^*$, which means that $h = x_3 + ix_3^*$ gives a global conformal parametrization of M . In the sequel, we will use this parametrization from \mathbb{C} into M , so that $h(z) = z$. Since $dh = dz$ has no zeros, we conclude that the Gauss map g misses $0, \infty$ on the entire surface M . Since M is simply connected, then g lifts through the natural exponential map $e^w: \mathbb{C} \rightarrow \mathbb{C}^*$ and thus, $g(z) = e^{H(z)}$ for some entire function H .

The next arguments show that H is a linear function of z , which clearly implies that M is a helicoid (recall that the only associate surface⁶ to the helicoid which is embedded as a mapping is the helicoid itself). Suppose H is not a linear function and we will obtain a contradiction. Applying Sard's theorem to the third component N_3 of the spherical Gauss map of M , we

⁶An associate surface to M with Weierstrass data (g, dh) is any of the (in general, multivalued) immersions with Weierstrass data $(g, e^{i\theta} dh)$, where $\theta \in [0, 2\pi)$.

deduce that there exists a latitude $\gamma \subset \mathbb{S}^2$ arbitrarily close to the horizontal equator, such that $g^{-1}(\gamma)$ does not contain any branch point of N_3 . Therefore, $g^{-1}(\gamma)$ consists of a proper collection of smooth curves. Note that there are no compact components in $g^{-1}(\gamma)$ since M is simply connected and g misses $0, \infty$. Also note that $H|_{g^{-1}(\gamma)}$ takes values along a certain line $l \subset \mathbb{C}$ parallel to the imaginary axis, and the restriction of H to every component of $g^{-1}(\gamma)$ parameterizes monotonically an arc in the line l . Hence, Picard's theorem implies that either H is a polynomial of degree $m \geq 2$ and $g^{-1}(\gamma)$ has m components, or $g^{-1}(\gamma)$ has an infinite number of components (equivalently, H is entire with an essential singularity at ∞).

The remainder of the proof breaks up into Cases A, B below. Each of these cases uses results of Colding and Minicozzi from [7] on the geometry of M . By the one-sided curvature estimates of Colding and Minicozzi [7], there exists a solid vertical hyperboloid of revolution $\mathcal{H} = \mathcal{H}(\delta, R) \subset \mathbb{R}^3$ (defined by (7)) such that $M - \mathcal{H}$ consists of two infinite valued graphs whose norms of their gradients are less than one. In particular, the curves in $g^{-1}(\gamma)$, when considered to be in the surface $M \subset \mathbb{R}^3$, are contained in \mathcal{H} . In Case B below, where H is a polynomial of degree $m \geq 2$ and $g^{-1}(\gamma)$ has m components, we may assume that at least one of the two ends of \mathcal{H} , say the top end, contains at least two of the ends of curves in $g^{-1}(\gamma)$. In Case A, where $g^{-1}(\gamma)$ is an infinite proper collection of curves inside \mathcal{H} , then at least one of the two ends of \mathcal{H} , say the top end, must contain an infinite number of ends of curves in $g^{-1}(\gamma)$. Thus in Case A for every $m \in \mathbb{N}$, there exists a large $T = T(m) > 0$ such that every plane $P_t = \{x_3 = t\}$ with $t > T(m)$ intersects at least m of the curves in $g^{-1}(\gamma)$.

Case A: $g^{-1}(\gamma)$ has an infinite number of components.

Using the rescaling argument in the proof of Proposition 5.2 (page 754) of [19], we can produce a blow-up limit $\widetilde{M} = \lim_k \lambda_k(M - p_k)$ of M that is a properly embedded, simply connected minimal surface with infinite total curvature and bounded Gaussian curvature; with some more detail, the points $p_k \in M$ are points of nonzero Gaussian curvature, the limit surface \widetilde{M} passes through the origin with this point as a maximum of its absolute Gaussian curvature, $\lim_{k \rightarrow \infty} x_3(p_k) = \infty$ and the intersection of \widetilde{M} with $\{x_3 = 0\}$ corresponds to the limit of scalings of the intersections of M with the sequence of planes P_{t_k} with $t_k = x_3(p_k) \rightarrow \infty$ and P_{t_k} intersects at least k components of $g^{-1}(\gamma)$. The new surface \widetilde{M} has the same appearance as that of M with two infinite valued graphs. In particular, if \widetilde{g} is the Gauss map of \widetilde{M} , then $\widetilde{g}^{-1}(\gamma)$ consists of a proper collection of curves which is contained in the related solid hyperboloid $\widetilde{\mathcal{H}}$ for \widetilde{M} . In particular, there are only a finite number of components of $\widetilde{g}^{-1}(\gamma)$ that intersect $\{x_3 = 0\}$, and we may also assume that γ is chosen so that $\widetilde{g}^{-1}(\gamma)$ intersects $\{x_3 = 0\}$ transversely in a finite number n_0 of points. By the extension property in [4], the related multivalued graphs in the domains $p_k + \frac{1}{\lambda_k} [\widetilde{M} \cap (\mathbb{R}^3 - \widetilde{\mathcal{H}})]$ near p_k extend with the norms of gradients at most 2 all the way to infinity in \mathbb{R}^3 (we used a similar argument in the sentence just before the statement of Lemma 3.2). Therefore, each of the infinitely many components of $g^{-1}(\gamma)$ must intersect transversely the plane $\{x_3 = x_3(p_k)\}$ in the compact disk $p_k + \frac{1}{\lambda_k} [\{x_3 = 0\} \cap \widetilde{\mathcal{H}}]$ for k sufficiently large. In particular, since $\widetilde{g}^{-1}(\gamma)$ intersects $\{x_3 = 0\}$ transversely in n_0 points, we find that $g^{-1}(\gamma)$ must have at most n_0 components, which is a contradiction. This contradiction implies that Case A does not occur.

Case B: H is a polynomial of degree $m \geq 2$ and $g^{-1}(\gamma)$ has m components.

Again using the rescaling argument in the proof of Proposition 5.2 of [19], we produce a simply connected minimal surface $\widetilde{M} = \lim_k \lambda_k(M - p_k)$ with infinite total curvature and absolute Gaussian curvature at most 1 and equal to 1 at $\vec{0} \in \widetilde{M}$, and with the property that the intersection of \widetilde{M} with $\{x_3 = 0\}$ corresponds to the limit of intersections of M with a sequence of planes P_{t_k} with $t_k = x_3(p_k) \rightarrow \infty$. As in Case A above, \widetilde{M} has the same appearance as that of M with two infinitely valued graphs, and if \tilde{g} denotes the Gauss map of \widetilde{M} , then $\tilde{g}^{-1}(\gamma)$ consists of a finite number of curves, each of which is contained in the related solid hyperboloid $\widetilde{\mathcal{H}}$ for \widetilde{M} . The same arguments as in the beginning of this proof of Theorem 4.1 demonstrate that the conformal type of \widetilde{M} is \mathbb{C} and \widetilde{M} can be conformally parameterized in \mathbb{C} with height differential dz and Gauss map $\tilde{g}(z) = e^{\tilde{H}(z)}$, for some entire function \tilde{H} .

We now show how the fact that \widetilde{M} has bounded Gaussian curvature gives that \tilde{H} is linear (and so, \widetilde{M} is a helicoid): Since the arguments in Case A above can be applied to \widetilde{M} , we conclude that \tilde{H} cannot have an essential singularity at $z = \infty$ and thus, \tilde{H} is a polynomial. Suppose that \tilde{H} has degree strictly greater than one, and we will get a contradiction. As $\tilde{g}(z)$ is an entire function with an essential singularity at ∞ and \tilde{g} misses $0, \infty$ (by the open mapping property since g also omits $0, \infty$), then \tilde{g} takes any value in $\mathbb{C} - \{0\}$ infinitely often in any punctured neighborhood of $z = \infty$. Thus, there exists a sequence $z_k \in \mathbb{C}$ diverging to ∞ as $k \rightarrow \infty$, such that $\tilde{g}(z_k) = 1$ for all k . Recall that the Gaussian curvature \tilde{K} of \widetilde{M} in terms of its Weierstrass data $(\tilde{g}(z) = e^{\tilde{H}(z)}, dz)$ is given by

$$\tilde{K} = -16|\tilde{H}'|^2 \frac{|\tilde{g}|^4}{(1 + |\tilde{g}|^2)^4};$$

hence $\tilde{K}(z_k) = -|\tilde{H}'(z_k)|^2$ tends to $-\infty$ as $k \rightarrow \infty$, which is a contradiction. This contradiction proves that \tilde{H} is linear and so, \widetilde{M} is a vertical helicoid.

Finally, the extension property in [4] implies that the related horizontal multivalued graphs in the domains $p_k + \frac{1}{\lambda_k} [\widetilde{M} \cap (\mathbb{R}^3 - \widetilde{\mathcal{H}})]$ near p_k extend all the way to infinity as multivalued graphs with the norm of the gradient less than 2. Reasoning as in the proof of Case A, for k large, $g^{-1}(\gamma)$ intersects transversely the plane $\{x_3 = x_3(p_k)\}$ in a subset of the compact disk $p_k + \frac{1}{\lambda_k} [\{x_3 = 0\} \cap \widetilde{\mathcal{H}}]$ that consists of a single point near p_k , since on the helicoid $\widetilde{\mathcal{H}}$, $\tilde{g}^{-1}(\gamma)$ is a helix or a vertical line that intersects the plane $\{x_3 = 0\}$ transversely in a single point. But by our choices, the top end of \mathcal{H} contains at least two ends of $g^{-1}(\gamma)$, each of which must intersect transversely the plane $\{x_3 = x_3(p_k)\}$ for k large. This is a contradiction which completes the proof of Case B, and so, it also finishes the proof of the theorem. \square

The next result is an immediate consequence of Theorem 4.1 and of the discussion before the statement of Proposition 3.4; also see the related rescaling argument in the proof of Proposition 5.2 of [19].

Corollary 4.2 *Let $M \subset \mathbb{R}^3$ be a complete, embedded minimal annulus and $X: D(R, \infty) \rightarrow \mathbb{R}^3$ be a conformal parametrization of M with Weierstrass data*

$$(g(z) = z^k e^{H(z)}, dh = dx_3 + i dx_3^*),$$

where $H(z)$ is holomorphic, dh has no zeroes in $D(R, \infty)$ and dh extends holomorphically across ∞ with a double pole at ∞ . Then, there exists positive numbers δ, R and sequences $\{p_n^+\}_{n \in \mathbb{N}}, \{p_n^-\}_{n \in \mathbb{N}}$ in $M \cap \mathcal{H}(\delta, R)$, $\{\lambda_n^+\}_{n \in \mathbb{N}}, \{\lambda_n^-\}_{n \in \mathbb{N}} \subset (0, \infty)$ such that:

1. $g(p_n^+) = g(p_n^-) = 1 \in \mathbb{C}$ for all $n \in \mathbb{N}$, and $x_3(p_n^+) \rightarrow \infty$, $x_3(p_n^-) = -\infty$ as $n \rightarrow \infty$.
2. The surfaces $\lambda_n(M - p_n^+)$ converge smoothly on compact subsets of \mathbb{R}^3 as $n \rightarrow \infty$ to a vertical helicoid $\mathbf{H} \subset \mathbb{R}^3$ which contains the x_3 and the x_2 -axes.

5 The Weierstrass representation of embedded minimal surfaces of finite topology.

In this section we describe an improvement of the analytic description of a complete injective minimal immersion of $\mathbb{S}^1 \times [0, \infty)$ into \mathbb{R}^3 that was given in Proposition 3.4. This improvement is given in the next theorem, which implies that M has finite type. Theorem 4 in [11] states that a complete, embedded minimal annular end of finite type with Weierstrass data as given in the next theorem and with zero flux, is asymptotic to the end of a vertical helicoid. We will prove this last fact again, independently, later with the stronger result described in Theorem 7.1. Note that if M has zero flux, then the number λ in item 2 below is zero and so, the next theorem will complete the proof of Theorem 1.1 except for item 3c; this item will follow from items 7, 8 of Theorem 7.1.

Theorem 5.1 *Suppose $M \subset \mathbb{R}^3$ is a complete, injectively immersed minimal annulus with compact boundary and infinite total curvature. After a homothety and rotation, M contains a subend M' with the following Weierstrass data:*

$$\left(g(z) = e^{iz+f(z)}, dh = \left(1 + \frac{\lambda}{z-\mu} \right) dz \right), \quad z \in D(\infty, R),$$

where $R > 0$, $f: D(\infty, R) \cup \{\infty\} \rightarrow \mathbb{C}$ is holomorphic with $f(\infty) = 0$, $\lambda \in [0, \infty)$ and $\mu \in \mathbb{C}$.

Proof. After a rotation of M and a replacement by a subend, we may assume by Proposition 3.4 that M is the image of a conformal minimal embedding $X: D(\infty, 1) \rightarrow \mathbb{R}^3$, the meromorphic Gauss map of X is equal to $g(z) = z^k e^{H(z)}$ where $k \in \mathbb{Z}$ and $H: D(\infty, 1) \rightarrow \mathbb{C}$ is some holomorphic function, and the holomorphic height differential of X is the one-form $dh = dx_3 + idx_3^*$ which has no zeroes and which extends meromorphically to $D(\infty, 1) \cup \{\infty\}$ with a double pole at infinity.

Assertion 5.2 *In the situation above, $k = 0$.*

Proof. Since $g(z) = z^k e^{H(z)}$, then k is the winding number of $g|_{\partial D(\infty, 1)}$ in $\mathbb{C} - \{0\}$. We will show that the winding number of $g|_{\partial D(\infty, 1)}$ is zero by proving that there exists a simple closed curve $\Gamma \subset D(\infty, 1)$ that is the boundary of an end representative of $D(\infty, 1)$ and such that $g|_\Gamma$ has winding number 0; since such a simple closed curve Γ is homotopic to $\partial D(\infty, 1)$, it will follow that the winding number of $g|_{\partial D(\infty, 1)}$ also vanishes.

By Proposition 3.4, there exist $R', h' > 0$ such that $M' = M - \text{Int}(C(R', h'))$ is a subend of M , each horizontal plane $P_t = \{x_3 = t\}$ intersects M' transversely in either a proper curve (if $|t| \geq h'$) or in two proper arcs, each with its single end point on the boundary of M' (if $|t| < h'$). By Corollary 4.2, there exist $\delta, R_1 > 0$ and a point $p^- \in M \cap \mathcal{H}(\delta, R_1)$ with

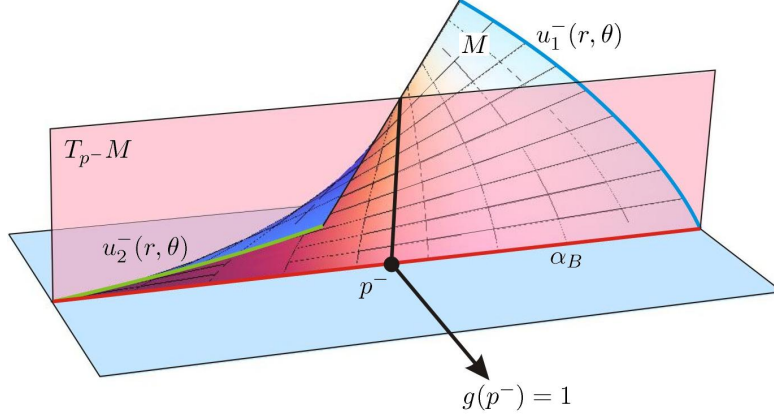


Figure 3: Around p^- , M has the appearance of a translated and homothetically shrunk vertical helicoid, made of two multivalued graphs $u_i^-(r, \theta)$, $i = 1, 2$.

$x_3(p^-) \ll -1$ such that $g(p^-) = 1$ and M has the appearance of a vertical helicoid around p^- . By the extension property in [4], the two resulting multivalued graphs in M around p^- extend indefinitely sideways as very flat multivalued graphs. Consider the intersection of M with the tangent plane $T_{p^-}M$. This intersection is an analytic 1-dimensional complex which contains an almost horizontal proper smooth curve α_B passing through p^- , which we may assume is globally parameterized by its x_2 -coordinate. In this case, α_B near p^- plays the role of the x_2 -axis contained in the helicoid \mathbf{H} that appears in Corollary 4.2. It follows that close to p^- , the argument of $g(z)$ on α_B can be chosen to be close to zero, see Figure 3.

Since the two horizontal multivalued graphs around p^- extend horizontally all the way to infinity in \mathbb{R}^3 , our earlier discussion before the statement of Proposition 3.4 implies that the related multivalued graphing functions u_1^-, u_2^- with polar coordinates centered at p^- , satisfy $\frac{\partial u_i^-}{\partial \theta} > 0$ for $i = 1, 2$ when restricted to $\alpha_B - \{p^-\}$, even at points far from the forming helicoid at p^- . Thus, if we consider the argument of the complex number $g(p^-)$ to lie in $(-\frac{\pi}{2}, \frac{\pi}{2})$, we conclude that the argument of $g(\alpha_B(t))$ also lies in $(-\frac{\pi}{2}, \frac{\pi}{2})$ for all $t \in \mathbb{R}$.

A similar discussion shows that there is a point $p^+ \in M \cap \mathcal{H}(\delta, R_1)$ with $x_3(p^+) \gg 1$ and a related almost horizontal curve $\alpha_T \subset M \cap T_{p^+}M$ passing through p^+ and such that the argument of g along α_T also takes values in the interval $(2\pi j - \frac{\pi}{2}, 2\pi j + \frac{\pi}{2})$, when we consider the argument of $g(p^+) = 1$ to lie in the interval $(2\pi j - \frac{\pi}{2}, 2\pi j + \frac{\pi}{2})$ for some $j \in \mathbb{N}$.

Recall from the discussion just before Proposition 3.4 that the hyperboloid $\mathcal{H}' = \mathcal{H}(\delta, R_2)$ was chosen so that in the complement of \mathcal{H}' , M consists of two multivalued graphs G'_1, G'_2 , respectively given by functions $u_1(r, \theta), u_2(r, \theta)$, such that $\frac{\partial u_i}{\partial \theta}(r, \theta) > 0$, $i = 1, 2$. Now can choose r' sufficiently large so that:

- The portion of $\alpha_T \cup \alpha_B$ outside of the solid vertical cylinder $C(r') = \{x_1^2 + x_2^2 \leq (r')^2\}$ consists of four connected arcs in $G'_1 \cup G'_2$, and the portion of $\alpha_T \cup \alpha_B$ inside $C(r')$ consists of two compact arcs $\alpha_T^{r'}, \alpha_B^{r'}$.
- $\partial C(r') \cap (G'_1 \cup G'_2)$ contains two connected spiraling arcs β_1, β_2 , each of which connects one end point of $\alpha_T^{r'}$ with one end point of $\alpha_B^{r'}$.

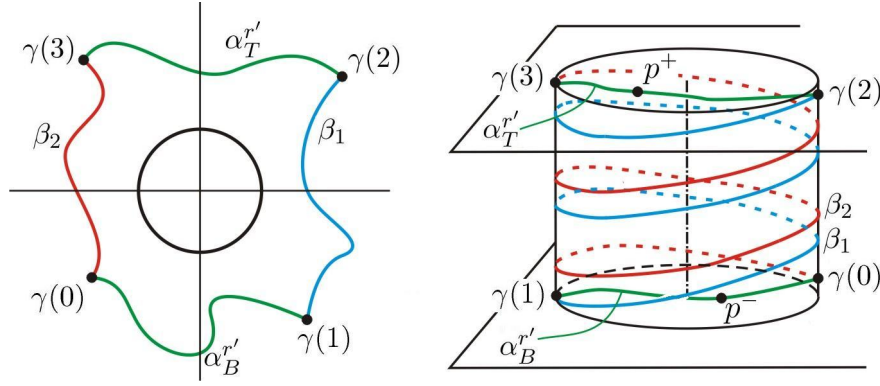


Figure 4: Left: The closed curve $\Gamma = \alpha_B^{r'} \cup \beta_1 \cup \alpha_T^{r'} \cup \beta_2$ is homotopic to the boundary of $D(\infty, 1)$. Right: The same loop Γ , viewed in $M \subset \mathbb{R}^3$; note that $\alpha_B^{r'}, \alpha_T^{r'}$ are contained in vertical planes parallel to the (x_2, x_3) -plane ($\alpha_B^{r'}, \alpha_T^{r'}$ are not necessarily contained in horizontal planes).

We define the simple closed curve $\Gamma = \alpha_B^{r'} \cup \beta_1 \cup \alpha_T^{r'} \cup \beta_2 \subset M$, see Figure 4. Note that Γ bounds a subend of M , and that Γ can be parameterized by a mapping $\gamma: [0, 4] \rightarrow \Gamma$, so that

- $\alpha_B^{r'}$ has end points $\gamma(0), \gamma(1)$,
- $\gamma(1), \gamma(2)$ are the end points of β_1 ,
- $\gamma(2), \gamma(3)$ are the end points of $\alpha_T^{r'}$, and
- β_2 has end points $\gamma(3), \gamma(4) = \gamma(0)$, see Figure 4 left.

Notice that the condition $\frac{\partial u_i}{\partial \theta}(r, \theta) > 0$ along $\beta_1 \cup \beta_2$ implies that the argument of $g(z)$ along β_1 , which we can choose to have an initial value at $\gamma(1) = \beta_1 \cap \alpha_B^{r'}$ in the interval $(-\frac{\pi}{2}, \frac{\pi}{2})$, has its value at $\gamma(2)$ in $(2\pi n - \frac{\pi}{2}, 2\pi n + \frac{\pi}{2})$, where n is the number of θ -revolutions that β_1 makes around the x_3 -axis (when we assume that the Gauss map of M is upward pointing along β_1). Similarly, the argument of $g(z)$ along β_2 , which has an initial value in $(2\pi n - \frac{\pi}{2}, 2\pi n + \frac{\pi}{2})$, has its ending value in $(-\frac{\pi}{2}, \frac{\pi}{2})$; we are using here the earlier observation that if the argument of $g(z)$ at one end point of α^T or α^B lies in $(2\pi m - \frac{\pi}{2}, 2\pi m + \frac{\pi}{2})$ for some $m \in \mathbb{N}$, then the other end point of the same α -curve also lies in $(2\pi m - \frac{\pi}{2}, 2\pi m + \frac{\pi}{2})$. It follows now that the winding number of $g|_\Gamma$ is zero, which completes the proof of the assertion. \square

We continue with the proof of Theorem 5.1. So far we have deduced that M can be parameterized by $D(\infty, 1)$ with Weierstrass data $g(z) = e^{H(z)}$, $H(z)$ holomorphic on $D(\infty, 1)$ and $dh = dx_3 + idx_3^*$, where dh has no zeroes and extends to $D(\infty, 1) \cup \{\infty\}$ with a double pole at infinity. We claim that $H(z) = P(z) + f(z)$, where $P(z)$ is a polynomial of degree one and $f(z)$ extends to a holomorphic function on $D(\infty, 1) \cup \{\infty\}$ with $f(\infty) = 0$. The first case we consider, Case A, is when $H(z)$ has an essential singularity at ∞ . This case cannot occur by the same arguments as those given in the proof of Theorem 4.1 in the similar Case A. The second case we consider, Case B, is when $H(z) = P(z) + f(z)$ where $P(z)$ is a polynomial of degree $m \geq 2$ and $f(\infty) = 0$. In this case the arguments of the related Case B in the proof of Theorem 4.1 show that this case cannot occur either. This proves the claim that

$H(z) = cz + d + f(z)$ where $c, d \in \mathbb{C}$ and $f(\infty) = 0$. Since M is assumed to have infinite total curvature, its Gauss map takes on almost all values of \mathbb{S}^2 infinitely often, which means that $c \neq 0$.

Finally we will obtain the Weierstrass data that appears in the statement of Theorem 5.1. Since dh has a double pole at infinity, then after a change of variables of the type $z \mapsto zT(z)$ for a suitable holomorphic function $T(z)$ in a neighborhood of ∞ with $T(\infty) \in \mathbb{C} - \{0\}$, we can write $dh = (A_0 + \frac{\lambda}{w}) dw$, where $A_0 \in \mathbb{C} - \{0\}$ and $-2\pi\lambda \in \mathbb{R}$ is the vertical component of the flux vector of M along its boundary. After possibly rotating M in \mathbb{R}^3 by 180° about a horizontal line, we can assume $\lambda \geq 0$. After a homothety of M in \mathbb{R}^3 and a suitable rotation $w \mapsto e^{i\theta}w$ in the parameter domain, we can prescribe A_0 in $\mathbb{C} - \{0\}$. As a rotation of M in \mathbb{R}^3 about the x_3 -axis does not change dh but multiplies g by a unitary complex number, then we can assume that the Weierstrass data of M are $g(w) = e^{cw+d+f(w)}$ and $dh = (-ic + \frac{\lambda}{w}) dw$. Finally, the linear change of variables $cw + d = i\xi$ produces $g(\xi) = e^{i\xi+f_1(\xi)}$, $dh = (1 + \frac{\lambda}{\xi+id}) d\xi$ where $f_1(\xi) = f(w)$. After choosing $R > 0$ sufficiently large, we have the desired Weierstrass data on $D(\infty, R)$. This concludes the proof of the theorem. \square

6 The analytic construction of the examples $E^{a,b}$.

In this section we will construct certain examples $E^{a,b}$ of complete *immersed* minimal annuli which depend on parameters $a, b \in [0, \infty)$ and so that their flux vector is $(a, 0, -b)$. The *embedded* canonical examples $E_{a,b}$ referred to in Theorem 1.3 will be end representatives of the corresponding examples $E^{a,b}$; this is explained in item 1 in Theorem 7.1 below. Our construction of the examples discussed in this section will be based on the classical Weierstrass representation. We first review how we can deduce the periods and fluxes of a potential minimal annulus from its Weierstrass representation.

Consider a meromorphic function g and a holomorphic one-form dh on the punctured disk $D(\infty, R)$ centered at ∞ , for some $R > 0$. Suppose that $(|g| + |g|^{-1})|dh|$ has no zeros in $D(\infty, R)$. The period and flux along $\partial_R = \{|z| = R\}$ of the (possibly multivalued) unbranched minimal immersion $X: D(\infty, R) \rightarrow \mathbb{R}^3$ associated to the Weierstrass data (g, dh) are given by

$$\text{Per} + i \text{Flux} = \frac{1}{2} \left(\int_{\partial_R} \frac{dh}{g} - \int_{\partial_R} g dh, i \int_{\partial_R} \frac{dh}{g} + i \int_{\partial_R} g dh, 0 \right) + \left(0, 0, \int_{\partial_R} dh \right) \in \mathbb{C}^3.$$

If we assume that the period of X vanishes, i.e. (6) holds, then the above formula gives

$$\text{Flux} = \left(-\text{Im} \int_{\partial_R} g dh, \text{Re} \int_{\partial_R} g dh, \text{Im} \int_{\partial_R} dh \right) \equiv \left(i \int_{\partial_R} g dh, \text{Im} \int_{\partial_R} dh \right) \in \mathbb{C} \times \mathbb{R}, \quad (8)$$

where we have identified \mathbb{R}^3 with $\mathbb{C} \times \mathbb{R}$ by $(a_1, a_2, a_3) \equiv (a_1 + ia_2, a_3)$.

It is clear that the choice $g(z) = e^{iz}$, $dh = dz$ produces the end of a vertical helicoid. In this section, we will consider explicit expressions for (g, dh) such that

1. $g(z) = e^{iz+f(z)}$, where $f: D(\infty, R) \cup \{\infty\} \rightarrow \mathbb{C}$ is holomorphic and $f(\infty) = 0$.
2. $dh = (1 + \frac{\lambda}{z-\mu}) dz$, where $\lambda \in [0, \infty)$ and $\mu \in \mathbb{C}$,

in terms of certain parameters defining $f(z)$ and μ and we will prove that these parameters can be adjusted so that the period problem for (g, dh) is solved, thereby defining a complete immersed minimal annulus $E^{a,b}$; furthermore, the flux vector of the resulting minimal immersion is $F = (a, 0, -b)$ and this vector can be chosen for every $a, b \geq 0$. In the particular case $a = b = 0$, we choose $f = \lambda = 0$; hence $E^{0,0}$ is the end of a vertical helicoid. The argument for the construction of the remaining annuli $E^{a,b}$ breaks up into two cases, depending on whether the flux vector F is vertical or not.

Case 1: The flux is not vertical.

Consider the following particular choice of g, dh :

$$g(z) = t e^{iz} \frac{z - A}{z}, \quad dh = \left(1 + \frac{B}{z}\right) dz, \quad z \in D(\infty, R), \quad (9)$$

where $t > 0$, $A \in \mathbb{C} - \{0\}$, $B \in [0, \infty)$ and $R > |A|$ are to be determined. Note that g can be rewritten as $g(z) = t e^{iz+f(z)}$ where $f(z) = \log \frac{z-A}{z}$, which is univalued and holomorphic in $D(\infty, R)$ since $R > |A|$. Furthermore, $f(\infty) = 0$. Also note that $\int_{\partial_R} dh = -2\pi i B$ is purely imaginary since $B \in \mathbb{R}$ (here ∂_R is oriented as boundary of $D(\infty, R)$). Therefore, the period problem for (g, dh) given by equation (6) reduces to the horizontal component. To study this horizontal period problem, we first compute $\int_{\partial_R} g dh$ as the residue of a meromorphic one-form in $\{|z| \leq R\}$, obtaining

$$\int_{\partial_R} g dh = 2\pi i t (A - B + iAB). \quad (10)$$

Arguing analogously with $\int_{\partial_R} \frac{dh}{g}$ we have

$$\int_{\partial_R} \frac{dh}{g} = -2\pi i \frac{A + B}{t e^{iA}}. \quad (11)$$

Hence the period condition (6) reduces to the equation

$$t [A(1 + iB) - B] = \frac{\bar{A} + B}{t} e^{i\bar{A}}. \quad (12)$$

Next we will show that the period problem (12) can be solved in the parameters t, A, B with arbitrary values of the flux vector different from vertical (the case of vertical nonzero flux will be treated in Case 2 below, with a different choice of g, dh).

Let $A = x + iy$ with $x, y \in \mathbb{R}$, and rewrite equation (12) in the following two ways:

$$t^2 e^{-y} [A(1 + iB) - B] = (\bar{A} + B) e^{ix} \quad (13)$$

$$t^2 e^{-y} [(x - By - B) + i(Bx + y)] = [(x + B) - iy] e^{ix}. \quad (14)$$

We fix $B \geq 0$ and for $y \in \mathbb{R}$, define the following related \mathbb{C} -valued curves:

$$L(x) = (x - By - B) + i(Bx + y), \quad R(x) = [(x + B) - iy] e^{ix}, \quad (15)$$

that contain the information on the arguments of the complex numbers of the left- and right-hand sides of equation (14), provided they are nonzero. Observe that these curves depend on the parameter y .

Also note that

$$|L(x)|^2 = (1 + B^2)(x^2 + y^2) + B^2 - 2Bx + 2B^2y. \quad (16)$$

As $(1 + B^2)y^2 + 2B^2y \geq -\frac{B^4}{1+B^2}$ for all $y \in \mathbb{R}$, then (16) gives

$$|L(x)|^2 \geq (1 + B^2)x^2 + B^2 - 2Bx - \frac{B^4}{1 + B^2} = (1 + B^2) \left(x - \frac{B}{1 + B^2} \right)^2. \quad (17)$$

Since our goal is to prove that both $t > 0$, $A \in \mathbb{C} - \{0\}$ can be chosen so that the period problem (12) is solved for a given $B \in \mathbb{R}$, then in the sequel we will fix $B \geq 0$ and take $x = \operatorname{Re}(A)$ larger than some particular values; namely,

$$x > \frac{B}{1 + B^2}. \quad (18)$$

Thus, (17) gives that $L(x) \neq 0$ when x satisfies (18), and so, we can write $L(x)$ in polar coordinates as

$$L(x) = r_L(x)e^{i\theta_L(x)},$$

where $r_L(x)$ is the modulus of $L(x)$ and $\theta_L(x)$ is its argument, taking values in the interval $(-\pi, \pi]$. Note that $L(x)$ cannot lie in the closed third quadrant for any value of $x > \frac{B}{1+B^2}$ (if $B = 0$, then $L(x) = x + iy$ with $x > 0$ and this property is clear; while if $B > 0$, then either $L(x)$ has positive real part in which case $L(x)$ cannot lie in the closed third quadrant, or $x - By - B \leq 0$ and in this case $Bx + y \geq Bx + \frac{1}{B}(x - B) = \frac{B^2+1}{B}x - 1 > 0$ so $L(x)$ also does not lie in the third quadrant), i.e. $\theta_L(x) \in (-\frac{\pi}{2}, \pi)$ for all $x > \frac{B}{1+B^2}$.

Viewing $L(x)$ as a curve in \mathbb{R}^2 with parameter x satisfying (18), we have:

$$\left| \frac{d\theta_L}{dx}(x) \right| \leq \frac{|L'(x)|}{|L(x)|} \stackrel{(15)}{=} \frac{|1 + iB|}{|L(x)|} \stackrel{(17)}{\leq} \left| x - \frac{B}{1 + B^2} \right|^{-1}. \quad (19)$$

On the other hand, note that $R(x) = 0$ if and only if $x = -B$ and $y = 0$. Since we are assuming that x satisfies (18), then $R(x)$ cannot vanish so we can write

$$R(x) = r_R(x)e^{i\theta_R(x)}$$

in polar coordinates, where $\theta_R(x) = x + \theta_1(x)$ and $\theta_1(x) = \arg[(x + B) - iy]$, which lies in the interval $(-\frac{\pi}{2}, \frac{\pi}{2})$. Therefore,

$$\frac{d\theta_R}{dx}(x) = 1 + \frac{d\theta_1}{dx}(x) \geq 1 + \min_{y \in \mathbb{R}} \frac{y}{(B + x)^2 + y^2} = 1 - \frac{1}{2(B + x)}. \quad (20)$$

Comparing the expression $m = m(B, x) = 1 - \frac{1}{2(B+x)}$ in the right-hand side of (19) with the one at the right-hand side of (20), we deduce directly the following property.

Assertion 6.1 *Given $B \in [0, \infty)$, there exists $x_0 = x_0(B)$ satisfying (18) such that such that if $x \in (x_0, \infty)$, then $\frac{d\theta_L}{dx}(x) < \frac{d\theta_R}{dx}(x)$.*

We are now ready to find $A \in \mathbb{C}$ (given $B \in [0, \infty)$) such that the complex numbers $L(x)$, $R(x)$ in equation (12) have the same argument.

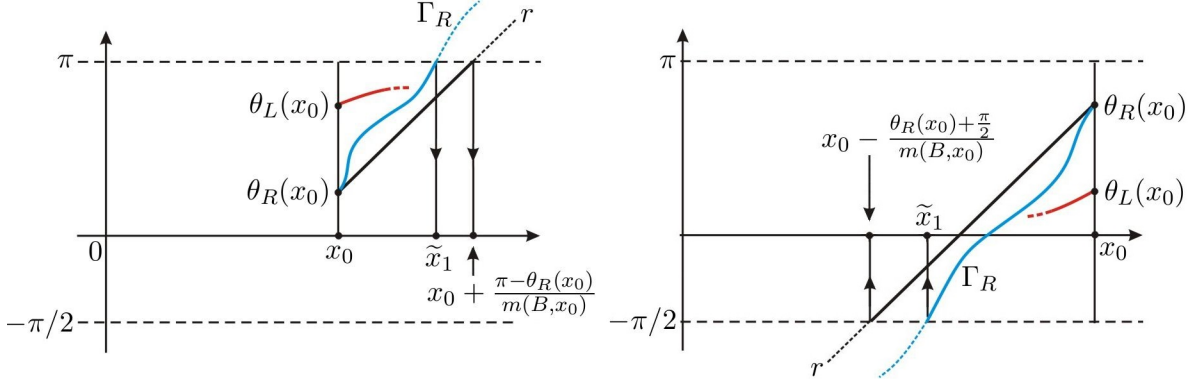


Figure 5: Left: Case A of Assertion 6.2; the half-line r has slope $m(B, x_0)$ very close to 1. The red and blue curves must intersect. Right: Case B of Assertion 6.2.

Assertion 6.2 *Given $B \geq 0$, we have one of the following two possibilities.*

- (A) *If $\theta_R(x_0) \leq \theta_L(x_0)$ (here $x_0 = x_0(B)$ refers to the value obtained in Assertion 6.1), then there exists a unique point $x_1 = x_1(B, y) \in I = \left[x_0, x_0 + \frac{\pi - \theta_R(x_0)}{m(B, x_0)} \right)$ such that $\theta_R(x_1) = \theta_L(x_1)$.*
- (B) *If $\theta_R(x_0) \geq \theta_L(x_0)$, then there exists a unique point $x_1 = x_1(B, y) \in I = \left(x_0 - \frac{\theta_R(x_0) + \frac{\pi}{2}}{m(B, x_0)}, x_0 \right]$ such that $\theta_R(x_1) = \theta_L(x_1)$.*

Furthermore, the function $(B, y) \mapsto x_1(B, y)$ is continuous.

Proof. Assume we are in case A, i.e., $\theta_R(x_0) \leq \theta_L(x_0)$. First note that by (20), the parameterized curve Γ_R given by $x \in [x_0, +\infty) \mapsto (x, \theta_R(x))$ lies entirely above the half-line r that starts at $(x_0, \theta_R(x_0))$ with slope $m(B, x_0)$ (this slope can be assumed arbitrarily close to 1 by taking x_0 large enough; note also that θ_R restricted to the half-open interval $[x_0, +\infty)$ is injective). By comparison of Γ_R with r , we easily conclude that θ_R must reach the value π at some point $\tilde{x}_1 > x_0$ which is not greater than $x_0 + \frac{\pi - \theta_R(x_0)}{m(B, x_0)}$, see Figure 5 left. Since the range of $x \in [x_0, \infty) \mapsto \theta_L(x)$ is $(-\frac{\pi}{2}, \pi)$, the intermediate value theorem applied to the function $\theta_R - \theta_L$ implies that there is at least one point $x_1 \in [x_0, \tilde{x}_1) \subset I$ such that $\theta_R(x_1) = \theta_L(x_1)$. Since $(\theta_R - \theta_L)'(x) > 0$ for all $x > x_0$ by Assertion 6.1, then the point $x_1 = x_1(B, y)$ is unique.

Case B can be proved with similar reasoning as in the last paragraph, using Figure 5 right instead of Figure 5 left (note that we need to apply Assertion 6.1 for values of x less than x_0 , which can be done by taking x_0 large enough). Finally, the continuous dependence of x_1 with respect to B, y follows from the same type of dependence for the data $\theta_L, \theta_R, x_0, m(B, x_0)$. This finishes the proof of the assertion. \square

Fix $B \in [0, \infty)$. Given $y \in \mathbb{R}$, consider the value $x_1 = x_1(B, y)$ appearing in Assertion 6.2 and let $A = x_1 + iy$. Since the left- and right-hand sides of equation (14) (with $x = x_1$, note that $t > 0$ is still to be determined) are not zero and the arguments of the complex numbers on each of the sides are the same, then there exists a unique $t = t(B, y) \in (0, \infty)$ varying

continuously in B, y so that equation (14) holds. Therefore, the period problem (12) is solved for the Weierstrass data (9) given by the values $B, A = x_1 + iy, t$. Let $E(B, y)$ denote the related minimally immersed annulus in \mathbb{R}^3 defined by these Weierstrass data. Let $F(B, y)$ denote the length of the horizontal flux of $E(B, y)$, which by equation (8) can be identified with the integral

$$F(B, y) = \left| \int_{\partial_R} g dh \right| \stackrel{(10)}{=} 2\pi t |(x_1 - By - B) + (Bx_1 + y)i|. \quad (21)$$

By equation (14) and the fact that $y \in \mathbb{R} \mapsto x_1(B, y)$ is bounded for B fixed (by Assertion 6.2), we see that $y \in \mathbb{R} \mapsto t(B, y)$ grows exponentially to ∞ as $y \rightarrow +\infty$ and decays exponentially to 0 as $y \rightarrow -\infty$. Hence, from (21) we also find:

$$\lim_{y \rightarrow +\infty} F(B, y) = \infty, \quad \lim_{y \rightarrow -\infty} F(B, y) = 0.$$

Since $y \in \mathbb{R} \mapsto F(B, y)$ is continuous, the intermediate value theorem proves the next assertion.

Assertion 6.3 *Given $B \in [0, \infty)$, the minimally immersed annuli $\{E(B, y) \mid y \in \mathbb{R}\}$ defined above attain all possible positive lengths for the horizontal component of their fluxes (the vertical component of their flux is always equal to $-2\pi B$). Hence, by the axiom of choice, for each $a > 0$ and $b \in [0, \infty)$, there exists $y = y(a, b) \in \mathbb{R}$ such that $E(\frac{b}{2\pi}, y(a, b))$ has vertical component of its flux equal to $-b$ and the length of the horizontal component of its flux is equal to a . After a rotation of $E(\frac{b}{2\pi}, y(a, b))$ around the x_3 -axis, we obtain the desired example $E^{a,b}$ with flux vector $(a, 0, -b)$.*

Case 2: The flux vector is vertical.

We now complete the construction of the canonical examples $E^{0,b}$, as complete immersed minimal annuli with infinite total curvature and flux vector $(0, 0, -b)$ for any $b \in (0, \infty)$. Fix $B \in (0, \infty)$ and consider the following choices for g, dh :

$$g(z) = e^{iz} \frac{z - A}{z - \bar{A}}, \quad dh = \left(1 + \frac{B}{z}\right) dz, \quad z \in D(\infty, R), \quad (22)$$

where $A \in \mathbb{C} - \{0\}$ and $R > |A|$. Our goal is to show that given $B > 0$, there exists A as before so that the Weierstrass data given by (22) solve the period problem (6) and define a complete immersed minimal annulus with infinite total curvature and flux vector $(0, 0, -2\pi B)$. Similarly as in Case 1, we can write g as $g(z) = e^{iz+f(z)}$ where $f(z) = \log \frac{z-A}{z-\bar{A}}$, which is univalent and holomorphic in $D(\infty, R)$ because $R > |A|$, and f extends to $z = \infty$ with $f(\infty) = 0$. The period problem (6) for (g, dh) reduces in this vertical flux case to

$$\int_{\partial_R} g dh = \int_{\partial_R} \frac{dh}{g} = 0. \quad (23)$$

We first compute $\int_{\partial_R} g dh$ in terms of residues of a meromorphic one-form in $\{|z| \leq R\}$ which we impose to be zero:

$$\int_{\partial_R} g dh = -2\pi i \left[e^{i\bar{A}} \left(\bar{A} - A + B - \frac{AB}{A} \right) + \frac{AB}{A} \right] = 0. \quad (24)$$

A direct computation shows that the integral $\int_{\partial_R} \frac{dh}{g}$ is the complex conjugate of the expression involving A, B in equation (24). Hence it suffices to find, given $B > 0$, a nonzero complex number A solving (24).

Multiplying equation (24) by \bar{A} and dividing by $-2\pi i$ yields:

$$e^{i\bar{A}} \left(\bar{A}^2 - |A|^2 + B(\bar{A} - A) \right) = -AB \quad (25)$$

Letting $A = x + iy$, we obtain

$$2ye^y e^{ix} [y + i(x + B)] = B(x + iy). \quad (26)$$

After fixing $y > 0$ and letting x vary in the range $\{1 < x < \infty\}$, we have that $1 < \frac{d\theta_L}{dx}(x)$ and $\frac{d\theta_R}{dx}(x) < 0$, where $\theta_L(x)$ and $\theta_R(x)$ denote the argument of the left- and right-hand sides of equation (26), both considered in the variable x . Also note that we can take branches of $\theta_R(x), \theta_L(x)$ so that $0 < \theta_R(x) < \frac{\pi}{2}$ for the range of values of x and y that we are considering and $\theta_L(2\pi - \frac{\pi}{2}) \in (-\frac{\pi}{2}, 0)$.

We define the interval $J = (2\pi - \frac{\pi}{2}, 2\pi + \frac{\pi}{2})$. It follows that given $B > 0$, for each $y > 0$ there is a unique $x = x(y) \in J$ such that the arguments of both sides of (26) are equal for $A = x(y) + iy$. Note that the norm of the left-hand side of (26), considered now to be a positive function of y , varies continuously with limit value 0 as y tends to 0^+ and $+\infty$ as $y \rightarrow \infty$, and this norm grows exponentially to $+\infty$ as $y \rightarrow \infty$. On the other hand, the norm of the right-hand side of (26) is bounded away from zero and grows linearly in y as y tends to $+\infty$. Thus, for any initial value $B > 0$, there exists $y \in \mathbb{R}^+$ and the corresponding $x = x(y) \in J$ such that the left- and right-hand sides of (26) are equal. This completes the proof of Case 2.

We can summarize this Case 2 in the next assertion. The proof of the last statement of this assertion follows from the observation that when the flux vector is $(0, 0, -b)$, then the Weierstrass data of the corresponding immersed minimal annulus $E^{0,b}$ is given by equation (22) with $B = \frac{b}{2\pi}$. It is easy to check that the conformal map $z \xrightarrow{\Phi} \bar{z}$ in the parameter domain $D(R, \infty)$ of $E^{0,b}$ satisfies $g \circ \Phi = 1/\bar{g}$, $\Phi^* dh = \bar{d}h$. Hence, after translating the surface so that the image of the point $R \in D(R, \infty)$ lies on the x_3 -axis, we deduce that Φ produces an isometry of $E^{0,b}$ which extends to a 180° -rotation of \mathbb{R}^3 around the x_3 -axis.

Assertion 6.4 *For any $b > 0$, there exists a constant $A \in \{x + iy \mid x \in J, y \in \mathbb{R}^+\}$ depending on b such that the corresponding Weierstrass data in (22) (with $B = \frac{b}{2\pi}$) define a minimally immersed annulus $E^{0,b}$ with flux vector $(0, 0, -b)$. Furthermore, the conformal map $z \rightarrow \bar{z}$ in the parameter domain $D(R, \infty)$ of $E^{0,b}$ extends to an isometry of \mathbb{R}^3 which is a 180° -rotation around the x_3 -axis.*

Finally, we can join Cases 1 and 2 to conclude the following main result of this section.

Assertion 6.5 *For each $a, b \geq 0$, there exists a complete, minimally immersed annulus $E^{a,b}$ defined on some $D(\infty, R)$, $R = R(a, b) > 0$ by the Weierstrass data*

$$\left(g(z) = e^{iz+f(z)}, \quad dh = \left(1 + \frac{1}{2\pi} \frac{b}{z - \mu} \right) dz \right),$$

where $f(z)$ is a holomorphic function in $D(\infty, R) \cup \{\infty\}$ with $f(\infty) = 0$, and $\mu \in \mathbb{C}$. Furthermore, the flux vector of $E^{a,b}$ along $\{|z| = R\}$ is $(a, 0, -b)$ and when $a = b = 0$, we choose $f(z) = 0$.

7 The proof of Theorem 1.3 and the embeddedness of the canonical examples $E_{a,b}$.

In Section 6 we focused on the Weierstrass representation of the surfaces under consideration. The actual surfaces themselves for given Weierstrass data are only determined up to a translation, because they depend on integration of analytic forms after making a choice of a base point z_0 in the parameter domain $\mathcal{D} \subset \mathbb{C}$. The parametrization of the surfaces is calculated as a path integral where the path begins at the base point. In the proof of the next theorem, the reader should remember that different choices of base points give rise to translations of the image minimal annulus that we are considering; the image point of the base point is always the origin $\vec{0} \in \mathbb{R}^3$.

Theorem 1.3 stated in the Introduction follows from the material described in the last section together with items 1, 5, 6, 7, 8 and 9 of the next theorem. Theorem 1.1 is also implied by the next statement. Recall that the remaining item 3c to be proved in Theorem 1.1 follows immediately from items 7, 8 below and the fact that $E_{0,0}$ can be taken to be the end of the vertical helicoid with Weierstrass data given by $g(z) = e^{iz}$, $dh = dz$. In item 6 below, we use the notation introduced just before the statement of Theorem 1.3.

The reader will find it useful to refer to Figure 1 in the Introduction for a visual geometric interpretation of some qualities of the complete, embedded minimal annulus E appearing in the next statement.

Theorem 7.1 *Suppose E is a minimally immersed annulus in \mathbb{R}^3 which is the image of a conformal immersion $X: D(\infty, R') \rightarrow \mathbb{R}^3$, with flux vector $(a, 0, -2\pi\lambda)$ for some $a, \lambda \geq 0$, whose Weierstrass data (g, dh) on $D(\infty, R')$ are given by*

$$\left(g(z) = e^{iz+f(z)}, dh = \left(1 + \frac{\lambda}{z-\mu} \right) dz \right),$$

where $f(z)$ is a holomorphic at ∞ with $f(\infty) = 0$, and $\mu \in \mathbb{C}$, $|\mu| < R'$. Then:

1. *For some $R_1 \geq R'$, X restricted to $D(\infty, R_1)$ is injective. In particular, each canonical example $E^{a,b}$ described in Assertions 6.3 and 6.4 contains an end representative $E_{a,b}$ which is a properly embedded minimal annulus with compact boundary and infinite total curvature.*
2. *The Gaussian curvature function K of X satisfies $\limsup_{R \rightarrow \infty} |K|_{X(D(\infty, R))} = 1$. In particular, K is bounded.*
3. *There exist $(x_T, y_T), (x_B, y_B) \in \mathbb{R}^2$ such that the image curves $X([R', \infty))$, $X((-\infty, -R'])$ are asymptotic to the vertical half-lines $r_T = \{(x_T, y_T, t) \mid t \in [0, \infty)\}$, $r_B = \{(x_B, y_B, t) \mid t \in (-\infty, 0]\}$ respectively.*
4. *$(x_T, y_T) - (x_B, y_B) = (0, -\frac{a}{2})$.*
5. *The sequences of translated surfaces $X_n = E - (0, 0, 2\pi n + \lambda \log n)$ and $Y_n = E + (0, 0, 2\pi n - \lambda \log n)$ converge respectively to right-handed vertical helicoids H_T, H_B where r_T is contained in the axis of H_T and r_B is contained in the axis of H_B . Furthermore, $H_B = H_T + (0, \frac{a}{2}, 0)$.*

6. After a fixed translation of E , assume that

$$(x_T, y_T) + (x_B, y_B) = (0, 0) \quad \text{and} \quad x_3(z) = x + \lambda \log |z - \mu|, \quad (27)$$

where x_3 is the third coordinate function of X and $z = x + iy$.

- a. There exists an $R_E > 1$ such that $E - C(R_E)$ consists of two disjoint multivalued graphs Σ_1, Σ_2 over $D(\infty, R_E) \subset \mathbb{R}^2$ of smooth functions $u_1, u_2: \tilde{D}(\infty, R_E) \rightarrow \mathbb{R}$ whose gradients with respect to the metric on $\tilde{D}(\infty, R_E)$ obtained by pulling back the standard flat metric in $D(\infty, R_E)$, satisfy $\nabla u_i(r, \theta) \rightarrow 0$ as $r \rightarrow \infty$.
- b. Consider the multivalued graphs $v_1, v_2: \tilde{D}(\infty, R_E) \rightarrow \mathbb{R}$ defined by

$$v_1(r, \theta) = \left(\theta + \frac{\pi}{2}\right) + \lambda \log \sqrt{\left(\theta + \frac{\pi}{2}\right)^2 + [\log(2r)]^2}, \quad (28)$$

$$v_2(r, \theta) = \left(\theta - \frac{\pi}{2}\right) + \lambda \log \sqrt{\left(\theta - \frac{\pi}{2}\right)^2 + [\log(2r)]^2}. \quad (29)$$

Then, for each $n \in \mathbb{N}$, there exists an $R_n > R_E$ such that $|u_i - v_i| < \frac{1}{n}$ in $\tilde{D}(\infty, R_n)$. In particular, for θ fixed and $i = 1, 2$, we have $\lim_{r \rightarrow \infty} \frac{u_i(r, \theta)}{\log(\log(r))} = \lambda$ (see Figure 1 and note that $b = 2\pi\lambda$ there).

c. Furthermore:

- I. When $a = 0$, then on $\tilde{D}(\infty, R_E)$ we have $|u_i - v_i| \rightarrow 0$ as $r + |\theta| \rightarrow \infty$.
- II. The separation function $w(r, \theta) = u_1(r, \theta) - u_2(r, \theta)$ converges to π as $r + |\theta| \rightarrow \infty$.

7. Suppose that $X_2: D(\infty, R_2) \rightarrow \mathbb{R}^3$ is another conformal minimal immersion with the same flux vector $(a, 0, -2\pi\lambda)$ as X and Weierstrass data (g_2, dh_2) given by

$$\left(g_2(z) = e^{iz+f_2(z)}, dh_2 = \left(1 + \frac{\lambda}{z - \mu_2}\right) dz\right)$$

where $f_2(z)$ is holomorphic at ∞ with $f_2(\infty) = 0$, and $\mu_2 \in \mathbb{C}$. Then, there exists a vector $\tau \in \mathbb{R}^3$ such that the $X_2(D(\infty, R_2)) + \tau$ is asymptotic to $E = X(D(\infty, R_1))$. In particular, for some translation vector $\hat{\tau} \in \mathbb{R}^3$, $E + \hat{\tau}$ is asymptotic to the canonical example $E_{a,b}$, where $b = 2\pi\lambda$. Note that if E and $E_{a,b}$ are each normalized by a translation as in (27), then E is asymptotic to $E_{a,b}$.

8. Given $(a, b) \neq (a', b') \in [0, \infty) \times [0, \infty)$, then, after any homothety and a rigid motion applied to $E_{a,b}$, the image surface is not asymptotic to $E_{a',b'}$.
9. Each of the canonical examples $E_{0,b}$ for $b \in \mathbb{R}$ is invariant under the 180° -rotation around the x_3 -axis l , and $l \cap E_{0,b}$ contains two infinite rays.

Proof. We will follow the ordering $2 \rightarrow 3 \rightarrow 4 \rightarrow 5 \rightarrow 6 \rightarrow 7 \rightarrow 8 \rightarrow 9 \rightarrow 1$ when proving the items in the statement of Theorem 7.1.

As f is holomorphic in a neighborhood of ∞ with $f(\infty) = 0$, the series expansion of f has only negative powers of z , so we can find $C > 0$ depending only on f such that

$$|f(z)| \leq C|z|^{-1}, \quad |f'(z)| \leq C|z|^{-2}, \quad \text{for any } z \in D(\infty, R'). \quad (30)$$

Throughout the proof, we will assume that $|C| \geq R'$. We will frequently refer to these two simple estimates for $f(z)$ and $f'(z)$.

We first prove item 2. The expression of the absolute Gaussian curvature $|K|$ of X in terms of its Weierstrass data is

$$|K| = \frac{16}{(|g| + |g|^{-1})^4} \frac{|dg/g|^2}{|dh|^2} = \frac{1}{[\cosh \operatorname{Re}(iz + f(z))]^4} \frac{|i + f'(z)|^2}{\left|1 + \frac{\lambda}{z - \mu}\right|^2}.$$

Since f is holomorphic in a neighborhood of ∞ with $f(\infty) = 0$, the last right-hand side is bounded from above, which easily implies item 2.

We next demonstrate item 3. Let $\gamma(r) = r$, $r \geq R'$, be a parametrization of the portion of the positive real axis in $D(\infty, R')$. We will check that $X \circ \gamma$ is asymptotic to a vertical half-line pointing up, which will be r_T ; the case of r_B follows from the same arguments, using $\gamma(r) = -r$. From the Weierstrass data of X , we have that for given real numbers T, R with $R' < R < T$:

$$\begin{aligned} (x_1 + ix_2)(T) - (x_1 + ix_2)(R) &= \frac{1}{2} \left(\int_R^T \frac{dh}{g} - \int_R^T g dh \right) \\ &= \frac{1}{2} \left(\int_R^T e^{-it-f(t)} \left(1 + \frac{\lambda}{t - \mu} \right) dt - \int_R^T e^{it+f(t)} \left(1 + \frac{\lambda}{t - \mu} \right) dt \right) \\ &= \frac{1}{2} \int_R^T e^{it} \left[e^{-\overline{f(t)}} \left(1 + \frac{\lambda}{t - \bar{\mu}} \right) - e^{f(t)} \left(1 + \frac{\lambda}{t - \mu} \right) \right] dt. \end{aligned} \quad (31)$$

Expanding the expression between brackets in the last displayed equation as a series in the variable t , we find

$$e^{-\overline{f(t)}} \left(1 + \frac{\lambda}{t - \bar{\mu}} \right) - e^{f(t)} \left(1 + \frac{\lambda}{t - \mu} \right) = -\frac{2\operatorname{Re}(C_1)}{t} + \mathcal{O}(t^{-2}),$$

where $f(t) = \frac{C_1}{t} + \mathcal{O}(t^{-2})$, $C_1 \in \mathbb{C} - \{0\}$ and $\mathcal{O}(t^{-2})$ denotes a function such that $t^2 \mathcal{O}(t^{-2})$ is bounded as $t \rightarrow \infty$. Hence, (31) yields

$$(x_1 + ix_2)(T) - (x_1 + ix_2)(R) = -\operatorname{Re}(C_1) \int_R^T \frac{e^{it}}{t} dt + \int_R^T e^{it} \mathcal{O}(t^{-2}) dt$$

Note that $\left| \int_R^T e^{it} t^{-2} dt \right| \leq \int_R^T t^{-2} dt = R^{-1} - T^{-1}$ which converges to R^{-1} as $T \rightarrow +\infty$. On the other hand, taking R, T of the form $R = \pi m$, $T = \pi n$ for large positive integers $m < n$, we have

$$\int_R^T \frac{e^{it}}{t} dt = \left(\sum_{k=1}^{n-m} \int_{\pi(m+k-1)}^{\pi(m+k)} \frac{\cos t}{t} dt \right) + i \left(\sum_{k=1}^{n-m} \int_{\pi(m+k-1)}^{\pi(m+k)} \frac{\sin t}{t} dt \right)$$

Both parenthesis in the last expression are partial sums of alternating series of the type $\sum_k (-1)^k a_k$ where $a_k \in \mathbb{R}^+$ converges monotonically to zero as $k \rightarrow \infty$. By the alternating series test, both series converge and we conclude that $(x_1 + ix_2)(T) - (x_1 + ix_2)(R)$ converges to a complex

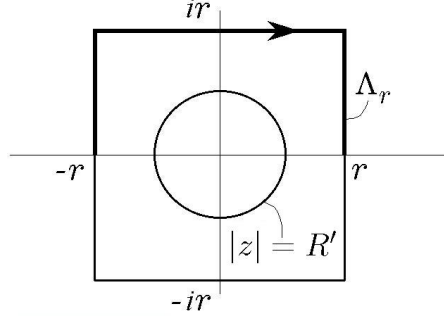


Figure 6: The square $\Lambda_2 - \overline{\Lambda_r}$ is homologous to the circle $\{|z| = R'\}$ in $D(\infty, R')$.

number as $T \rightarrow \infty$ (independent of R). As the third coordinate function of the immersion satisfies

$$x_3(T) - x_3(R) = \operatorname{Re} \int_R^T dh = T - R + \lambda \log \left| \frac{T - \mu}{R - \mu} \right|,$$

which tends to ∞ as $T \rightarrow \infty$, then we conclude that item 3 of the theorem holds.

We next prove item 4, which is equivalent to:

$$\lim_{r \rightarrow +\infty} [(x_1 + ix_2)(r) - (x_1 + ix_2)(-r)] = -\frac{ia}{2}. \quad (32)$$

To see that (32) holds, we use computations inspired by those in Section 5 of [11]. Take $r > R'$ and consider the boundary ∂S_r of the square $S_r \subset \mathbb{C}$ with vertices $r + ir, r - ir, -r - ir, -r + ir$. ∂S_r can be written as $\Lambda_r - \overline{\Lambda_r}$, where Λ_r is the polygonal arc with vertices $-r, -r + ir, r + ir, r$ (the orientations on ∂S_r and Λ_r are chosen so that both lists of vertices are naturally well-ordered, see Figure 6). As $\{|z| = R'\}$ and ∂S_r bound a compact domain in the surface, it follows that the horizontal component of the flux of X along ∂S_r equals $(a, 0)$. By equations (6) and (8), this is equivalent to the following equality:

$$\int_{\Lambda_r} \frac{dh}{g} = \int_{\overline{\Lambda_r}} \frac{dh}{g} + ia. \quad (33)$$

Hence,

$$\begin{aligned} (x_1 + ix_2)(r) - (x_1 + ix_2)(-r) &= \int_{\Lambda_r} d(x_1 + ix_2) = \frac{1}{2} \left(\int_{\Lambda_r} \frac{dh}{g} - \int_{\Lambda_r} g dh \right) \\ &\stackrel{(33)}{=} \frac{1}{2} \left(\int_{\overline{\Lambda_r}} \frac{dh}{g} - ia - \int_{\Lambda_r} g dh \right) = \frac{1}{2} (I_2 - I_1) + \frac{1}{2} (\widehat{I}_2 - \widehat{I}_1) - \frac{ia}{2}, \end{aligned}$$

where $I_1 = \int_{\Lambda_r} g dz$, $I_2 = \int_{\overline{\Lambda_r}} \overline{g}^{-1} d\overline{z}$, $\widehat{I}_1 = \int_{\Lambda_r} g \frac{\lambda}{z-\mu} dz$ and $\widehat{I}_2 = \int_{\overline{\Lambda_r}} \overline{g}^{-1} \frac{\overline{\lambda}}{\overline{z}-\mu} d\overline{z}$.

We now compute and estimate the norm of each of these four integrals separately. We first calculate I_1 and I_2 .

$$\begin{aligned} I_1 &= \int_0^r g(-r + iv) i dv + \int_{-r}^r g(u + ir) du - \int_0^r g(r + iv) i dv \\ &= e^{-r} \int_{-r}^r e^{iu+f(u+ir)} du + i \int_0^r e^{-v} \left(e^{-ir+f(-r+iv)} - e^{ir+f(r+iv)} \right) dv. \end{aligned}$$

If we take r such that $\frac{r}{2\pi}$ is integer, then I_1 becomes

$$I_1 = e^{-r} \int_{-r}^r e^{iu+f(u+ir)} du + i \int_0^r e^{-v} \left(e^{f(-r+iv)} - e^{f(r+iv)} \right) dv.$$

and a similar computation for I_2 gives

$$I_2 = e^{-r} \int_{-r}^r e^{iu-\overline{f(u-ir)}} du + i \int_0^r e^{-v} \left(e^{-\overline{f(-r-iv)}} - e^{-\overline{f(r-iv)}} \right) dv.$$

Thus, both I_1 and I_2 are sum of two integrals and each one of these four integrals can be estimated using (30) as follows:

$$\begin{aligned} \left| e^{-r} \int_{-r}^r e^{iu+f(u+ir)} du \right| &\leq e^{-r} \int_{-r}^r e^{\operatorname{Re}(f(u+ir))} du \\ &\leq e^{-r} \int_{-r}^r e^{C|u+ir|^{-1}} du \leq e^{-r} \int_{-r}^r e^{Cr^{-1}} du = 2re^{-r+Cr^{-1}}, \end{aligned}$$

and analogously, $\left| e^{-r} \int_{-r}^r e^{iu-\overline{f(u-ir)}} du \right| \leq 2re^{-r+Cr^{-1}}$, while

$$\left| i \int_0^r e^{-v} \left(e^{f(-r+iv)} - e^{f(r+iv)} \right) dv \right| \leq \int_0^r e^{-v} \left| e^{f(-r+iv)} - e^{f(r+iv)} \right| dv.$$

Using (30), it is straightforward to check that both $e^{f(-r+iv)}$ and $e^{f(r+iv)}$ can be expressed as $1 + \mathcal{O}(r^{-1})$, hence the last expression is of the type $\int_0^r e^{-v} \mathcal{O}(r^{-1}) dv \leq C_1 r^{-1} (1 - e^{-r})$, for a constant $C_1 > 0$ independent of r . Similarly, $\left| i \int_0^r e^{-v} \left(e^{-\overline{f(-r-iv)}} - e^{-\overline{f(r-iv)}} \right) dv \right| \leq C_1 r^{-1} (1 - e^{-r})$. Since the integrands of \hat{I}_1, \hat{I}_2 differ from the respective integrand of I_1, I_2 by a product with $\frac{\lambda}{z-\mu}$ and since $|\frac{\lambda}{z-\mu}| < 1$ for $|z|$ sufficiently large, then $|\hat{I}_1| < |I_1|, |\hat{I}_2| < |I_2|$, when r is large. In summary,

$$\left| (x_1 + ix_2)(r) - (x_1 + ix_2)(-r) + \frac{ia}{2} \right| \leq |I_2| + |I_1| \leq 2 \left[2re^{-r+Cr^{-1}} + C_1 r^{-1} (1 - e^{-r}) \right],$$

which tends to zero as $r \rightarrow +\infty$. This completes the proof that equation (32) holds and so proves item 4 of the theorem.

Next we prove item 5. For $n \in \mathbb{Z}, 2\pi n > R'$, let $D(n) = \{z \in \mathbb{C} \mid |z - 2\pi n| \leq 2\pi n - R'\}$ be the closed disk of radius $2\pi n - R'$ centered at $2\pi n$, and note that $D(n) \subset D(\infty, R')$. For $|n|$ large, consider the immersion $\tilde{X}_n: D(n) \rightarrow \mathbb{R}^3$ with the same Weierstrass data as X restricted to the disk $D(n)$, and with base point $2\pi n$ (in particular, \tilde{X}_n is a translation of a portion of X). The minimal immersions $\tilde{X}_n: D(n) \rightarrow \mathbb{R}^3$ converge uniformly to the right-handed vertical helicoid H with Weierstrass representation data $g(z) = e^{iz}, dh = dz, z \in \mathbb{C}$, and base point $\tilde{z}_0 = 0$. After letting $z_0 \in D(\infty, R')$ denote the base point of X , then the third coordinate

functions x_3 of X and $\tilde{x}_{3,n}$ of \tilde{X}_n are related by

$$\begin{aligned}
x_3(z) - 2\pi n + \operatorname{Re}(z_0) &= \operatorname{Re} \int_{z_0}^z \left(1 + \frac{\lambda}{z - \mu}\right) dz - 2\pi n + \operatorname{Re}(z_0) \\
&= \operatorname{Re}(z) + \lambda \log \left| \frac{z - \mu}{z_0 - \mu} \right| - 2\pi n \\
&= \int_{2\pi n}^z \left(1 + \frac{\lambda}{z - \mu}\right) dz + \lambda \log \left| \frac{2\pi n - \mu}{z_0 - \mu} \right| \\
&= \tilde{x}_{3,n}(z) + \lambda \log \left| \frac{2\pi n - \mu}{z_0 - \mu} \right| \\
&= \tilde{x}_{3,n}(z) + \lambda \log n + \lambda \log \left| \frac{2\pi - \frac{\mu}{n}}{z_0 - \mu} \right|.
\end{aligned}$$

Therefore, the minimal surfaces $X_n := E + (0, 0, -2\pi n - \lambda \log n)$ converge as $n \rightarrow \infty$ to a translated image $H_T := H + \tau$ of the helicoid H , where $\tau \in \mathbb{R}^3$ has vertical component $-\operatorname{Re}(z_0) + \lambda \log \frac{2\pi}{|z_0 - \mu|}$. Clearly, $r_T \subset r_T + (0, 0, -2\pi n - \lambda \log n)$ is contained in H_T . Similar computations give that the surfaces $E + (0, 0, 2\pi n - \lambda \log n)$ converge as $n \rightarrow \infty$ to a translated image $H_B := H + \tau'$ of H such that $x_3(\tau) = x_3(\tau')$. Now item 4 gives that $\tau - \tau' = (0, -\frac{a}{2}, 0)$, and item 5 holds.

Next we prove item 6. Throughout the proof of this item we will let

$$\Delta(n) = \{z = x + iy \in \mathbb{C} \mid |y| \geq n\},$$

where $n \in \mathbb{N}$. First translate E as required in the first sentence of item 6 of Theorem 7.1, and use the same notation X for the translated immersion which parameterizes E . Next observe that for some fixed large positive integer n_0 and for each $n \in \mathbb{N}$ with $n \geq n_0$, we have

(P1) $\partial D(\infty, R')$ is contained in the horizontal strip $\mathbb{C} - \Delta(n)$.

(P2) As $n \rightarrow \infty$, the Gaussian image of $X(\Delta(n))$ is contained in smaller and smaller neighborhoods of $(0, 0, \pm 1)$ in \mathbb{S}^2 , which converge as sets to the set $\{(0, 0, \pm 1)\}$ in the limit.

Property (P2) implies that E is locally graphical over its projection to the (x_1, x_2) -plane. We next study this locally graphical structure.

From the Weierstrass representation of X we conclude that for $z = x + iy \in D(\infty, R')$,

$$\begin{aligned}
(x_1 + ix_2)(z) &= \frac{1}{2} \left(\overline{\int^z \frac{dh}{g}} - \int^z g dh \right) \\
&= \frac{1}{2} \left(\overline{\int^z e^{-i\xi - f(\xi)} \left(1 + \frac{\lambda}{\xi - \mu}\right) d\xi} - \int^z e^{i\xi + f(\xi)} \left(1 + \frac{\lambda}{\xi - \mu}\right) d\xi \right) \\
&= \frac{1}{2} \left(\overline{\int^z e^{-i\xi} (1 + F_1(\xi)) d\xi} - \int^z e^{i\xi} (1 + F_2(\xi)) d\xi \right) \\
&= \frac{i}{2} (e^{iz} - e^{i\bar{z}}) + \frac{1}{2} (\overline{A_1(z)} - A_2(z)) \\
&= \frac{ie^{ix}}{2} (e^{-y} - e^y) + \frac{1}{2} (\overline{A_1(z)} - A_2(z)), \tag{34}
\end{aligned}$$

where $F_1(\xi), F_2(\xi)$ are holomorphic functions in $D(\infty, R') \cup \{\infty\}$ with $F_i(\infty) = 0, i = 1, 2$ (we are using that $f(z)$ is holomorphic at ∞ with $f(\infty) = 0$), and

$$A_1(z) = \int^z e^{-i\xi} F_1(\xi) d\xi, \quad A_2(z) = \int^z e^{i\xi} F_2(\xi) d\xi, \quad |z| \geq R'.$$

Since F_1, F_2 are holomorphic and vanish at infinity, we have the following technical assertion, which will be proven in the appendix (Section 8).

Definition 7.2 A complex valued function $E(z)$ defined in $D(\infty, R')$ is said to satisfy property \diamond if E is bounded and $|E(z)|$ can be made uniformly small by taking R' sufficiently large.

Assertion 7.3 There exist constants $C_1, C_2 > 0$ depending only on F_1, F_2 and complex valued functions $B_1(z), B_2(z)$ in $D(\infty, R')$ satisfying property \diamond , such that for all $z \in D(\infty, R')$,

$$|A_1(z) - B_1(z)| \leq \frac{C_1}{R'}(e^{|y|} - 1), \quad |A_2(z) - B_2(z)| \leq \frac{C_2}{R'}(1 - e^{-|y|}). \quad (35)$$

We come back to our study of the vertical projection of E . If $y \geq 0$, then the right-hand side of (34) can be written as $e^y \left(-\frac{ie^{ix}}{2} + D_1(z) \right)$, where $D_1(z) = \frac{e^{-y}}{2} \left(e^{-y} ie^{ix} + \overline{A_1(z)} - A_2(z) \right)$. In particular, the triangle inequality gives

$$\begin{aligned} |D_1(z)| &\leq \frac{e^{-y}}{2} \left(e^{-y} + \sum_{i=1}^2 |A_i(z) - B_i(z)| + \sum_{i=1}^2 |B_i(z)| \right) \\ &\stackrel{(35)}{\leq} \frac{e^{-y}}{2} \left(e^{-y} + \frac{C_1}{R'}(e^y - 1) + \frac{C_2}{R'}(1 - e^{-y}) + \sum_{i=1}^2 |B_i(z)| \right) = \frac{C_1}{2R'} + e^{-y} B_3(z), \end{aligned} \quad (36)$$

where $B_3(z)$ is a nonnegative function in $D(\infty, R')$ that satisfies property \diamond . A similar analysis can be done for $y \leq 0$, concluding that

$$(x_1 + ix_2)(z) = \begin{cases} e^y \left(-\frac{ie^{ix}}{2} + D_1(z) \right) & \text{if } y \geq 0, \\ e^{-y} \left(\frac{ie^{ix}}{2} + D_2(z) \right) & \text{if } y \leq 0, \end{cases} \quad (37)$$

where $z = x + iy$ and $D_2(z) = \frac{e^y}{2} \left(-e^y ie^{ix} + \overline{A_1(z)} - A_2(z) \right)$; in particular,

$$|D_2(z)| \leq \frac{C_2}{2R'} + e^y B_4(z), \quad (38)$$

where $B_4(z)$ is a nonnegative function in $D(\infty, R')$ that satisfies property \diamond .

Equation (37) implies that for $n \in \mathbb{N}$ large, $|(x_1 + ix_2)(z)| < 2e^n$ whenever $|y| \leq n$, from where $X(\mathbb{C} - \Delta(n)) \subset C(2e^n)$. Therefore, choosing $R_E = 2e^{n_0}$ with $n_0 \in \mathbb{N}$ large, we deduce from (37) that $E - C(R_E)$ consists of two disjoint multivalued graphs Σ_1, Σ_2 associated to smooth functions $u_1, u_2: \tilde{D}(\infty, R_E) \rightarrow \mathbb{R}$ (recall that $\tilde{D}(\infty, R_E)$ denotes the universal cover of $D(\infty, R_E)$), and that are defined by the equations

$$u_j(r, \theta) \stackrel{(27)}{=} x_3(z) = x + \lambda \log |z - \mu|, \quad (39)$$

where $x + iy = z = z(r, \theta)$ satisfies $y \geq 0$ if $j = 1$ (resp. $y \leq 0$ if $j = 2$) and

$$re^{i\theta} = \begin{cases} e^y \left(-\frac{ie^{ix}}{2} + D_1(z) \right) & \text{if } j = 1, \\ e^{-y} \left(\frac{ie^{ix}}{2} + D_2(z) \right) & \text{if } j = 2. \end{cases} \quad (40)$$

In particular, Σ_i is embedded, for $i = 1, 2$. Also, from (36), (38) and (40) we have that as functions of r, θ , the expressions of x, y are of the form

$$y = \log(2r) + \frac{b_1(r, \theta)}{R'}, \quad x = \begin{cases} \theta + \frac{\pi}{2} + \frac{b_2(r, \theta)}{R'} & \text{if } j = 1, \\ \theta - \frac{\pi}{2} + \frac{b_2(r, \theta)}{R'} & \text{if } j = 2, \end{cases} \quad (41)$$

where b_1, b_2 are bounded functions defined in $\tilde{D}(\infty, R_E)$. Plugging (41) into (39) we deduce that

$$\begin{aligned} u_1(r, \theta) &= x + \lambda \log |z| + \lambda \log \left| 1 - \frac{\mu}{z} \right| \\ &= \theta + \frac{\pi}{2} + \lambda \log \sqrt{\left(\theta + \frac{\pi}{2} \right)^2 + [\log(2r)]^2} + \frac{b_3(r, \theta)}{R'} \\ &= v_1(r, \theta) + \frac{b_3(r, \theta)}{R'}, \end{aligned} \quad (42)$$

where b_3 is a bounded function defined in $\tilde{D}(\infty, R_E)$ and v_1 is the multigraphing function defined in item 6b of Theorem 7.1. Analogously, the multigraphing function that defines Σ_2 verifies that $(u_2 - v_2)R'$ is bounded. Therefore, item 6b of Theorem 7.1 is proved.

As for the property $\nabla u_i(r, \theta) \rightarrow 0$ as $r \rightarrow \infty$ stated in item 6a of Theorem 7.1, it follows from standard gradient estimates once we know that around any point $re^{i\theta}$ in $D(\infty, R_E)$ with r sufficiently large, the boundary values of u_i in a disk of radius 1 centered at $re^{i\theta}$ are arbitrarily close to a constant value. This finishes the proof of item 6a of Theorem 7.1.

By item 4 and our translation normalization, if $a = 0$ then the rays r_T and r_B are contained in the x_3 -axis. By item 6b, $|u_i - v_i|$ can be made arbitrarily small if r is sufficiently large. Thus, in order to prove part I of item 6c, it suffices to show that $|u_i - v_i|$ tends to zero when r is bounded and $|\theta| \rightarrow \infty$. Consider the multigraph E' over $D(\infty, R_E)$ associated to the function v_i given by (28). The sequence of surfaces $E' - (0, 0, 2\pi n + \lambda \log n)$ can be seen to converge to the multigraph associated to the function $v_\infty(r, \theta) = \theta + \frac{\pi}{2} - \lambda \log(2\pi)$, which is contained in a vertical helicoid H' whose the axis is the x_3 -axis. As by item 5 the translated multigraphs $\Sigma_1 - (0, 0, 2\pi n + \lambda \log n)$ converge to a multigraph contained in the vertical helicoid H_T (which also contains x_3 -axis since H_T contains r_T), then to finish part I of item 6b it only remains to show that $H = H'$. This equality holds since $|u_i - v_i|(r, \theta)$ tends to zero as $r \rightarrow \infty$. Now part I of item 6b is proved.

As for part II of item 6b and regardless of the condition $a = 0$, the facts that the separation function between v_1 and v_2 has an asymptotic value of π as $r \rightarrow \infty$ together with the estimates in item 6b imply that the separation function $w(r, \theta) = u_1(r, \theta) - u_2(r, \theta)$ between u_1 and u_2 converges to π as $r \rightarrow \infty$. If r is bounded and $|\theta| \rightarrow \infty$, then the same limiting property for $w(r, \theta)$ holds by item 5, since the separation of the multigraphs in the helicoid H_B or in H_T is constant π . Now the proof of item 6 is complete.

Next we prove item 7. Suppose that $X_2: D(\infty, R_2) \rightarrow \mathbb{R}^3$ is another conformal minimal immersion with the same flux vector $(a, 0, -2\pi\lambda)$ as X and with Weierstrass data (g_2, dh_2) as

described in item 7. Since X, X_2 have the same flux vector, then item 4 allows us to find translations $Y_1 = E + \tau_1$ and $Y_2 = X_2(D(\infty, R_2)) + \tau_2$ of $E = X(D(\infty, R_1))$ and $X_2(D(\infty, R_2))$ respectively, such that Y_1, Y_2 each has the same half-axes projections $(x_T, y_T) = (0, -\frac{a}{4})$, $(x_B, y_B) = (0, \frac{a}{4})$. Now translate vertically Y_1, Y_2 so that their third coordinate functions are respectively given by

$$x_3(z) = x + \lambda \log |z - \mu|, \quad y_3(z) = x + \lambda \log |z - \mu_2|.$$

Thus, we can apply item 6b to Y_1, Y_2 and the corresponding functions v_1, v_2 in (28), (29) are the same for both Y_1, Y_2 . By transitivity we have that given any $n \in \mathbb{N}$, there is a large $R_n > 0$ such that each of the two multivalued graphs of $Y_1 - C(R_n)$ is $\frac{2}{n}$ -close to the corresponding multivalued graph of $Y_2 - C(R_n)$ in $\tilde{D}(\infty, R_n)$. Also, the proof of item 4 can be adapted to show that both $Y_1 - (0, 0, 2\pi n + \lambda \log n)$, $Y_2 - (0, 0, 2\pi n + \lambda \log n)$ both converge to the same vertical helicoid. Hence, Y_1 and Y_2 are asymptotic in \mathbb{R}^3 , and item 7 is proved.

Item 8 follows from the asymptotic description of an example E with flux vector $(a, 0, -b)$ given in 6 in terms of the flux components $a, b = 2\pi\lambda$. The symmetry property in item 9 follows directly from Assertion 6.4. Finally, item 1 on the embeddedness of some subend of E follows immediately from the asymptotic embeddedness information described in items 5 and 6, together with the next straightforward observation: Embeddedness of E outside of a vertical cylinder follows from the sentence just after equation (40) together with the positivity of the separation function given in part II of item 6c, while embeddedness inside a vertical cylinder and outside of a ball follows from item 5. \square

8 Appendix.

Proof of Assertion 7.3. We will denote by z_0 the (common) base point for the integration in the functions $A_i(z)$ (recall that Assertion 7.3 is only used in the proof of item 6 of Theorem 7.1, whose first sentence assumes that E has been translated as required in (27)). We decompose the integration path in $A_i(z)$ into three consecutive embedded arcs joined by their common end points: an arc Γ of the circle of radius $\{|z| = |z_0|\}$ from z_0 to a point R_0 in the positive or negative x -axis (we take R_0 with the same sign as $\operatorname{Re}(z)$), and two segments parallel to the x - and y -axes. This decomposition procedure works if $|\operatorname{Re}(z)| \geq |z_0|$; if on the contrary $|\operatorname{Re}(z)| < |z_0|$, then the decomposition can be changed in a straightforward manner taking R_0 in the y -axis, which does not affect essentially the arguments that follow.

Thus,

$$A_1(z) = \int_{\Gamma} e^{-i\xi} F_1(\xi) d\xi + \int_{R_0}^x e^{-iu} F_1(u) du + ie^{-ix} \int_0^y e^v F_1(x + iv) dv, \quad (43)$$

$$A_2(z) = \int_{\Gamma} e^{i\xi} F_2(\xi) d\xi + \int_{R_0}^x e^{iu} F_2(u) du + ie^{ix} \int_0^y e^{-v} F_2(x + iv) dv. \quad (44)$$

We define $B_1(z)$ (resp. $B_2(z)$) as the sum of the two first integrals in (43) (resp. in (44)). It remains to show that both B_1, B_2 satisfy property \diamond , and that the modulus of the third integral in (43) (resp. in (44)) satisfies the first inequality in (35) (resp. the second inequality).

As F_1, F_2 are holomorphic and vanish at ∞ , then $F_i(z) = \frac{C'_i}{z} + \frac{G_i(z)}{z^2}$ in $D(\infty, R')$, where $C'_i \in \mathbb{C}$ and G_i is holomorphic in $D(\infty, R') \cup \{\infty\}$. In particular, the first integral of each

of the right-hand sides of (43) and (44) define a complex constant (independent of z such that $|\operatorname{Re}(z)| \geq |z_0|$) that can be taken arbitrarily small if R' is sufficiently large. As for the second integral of (43), (44),

$$\int_{R_0}^x e^{-iu} F_1(u) du = C'_1 \int_{R_0}^x \frac{e^{-iu}}{u} du + \int_{R_0}^x \frac{e^{-iu}}{u^2} G_1(u) du, \quad (45)$$

$$\int_{R_0}^x e^{iu} F_2(u) du = C'_2 \int_{R_0}^x \frac{e^{iu}}{u} du + \int_{R_0}^x \frac{e^{iu}}{u^2} G_2(u) du. \quad (46)$$

To study the first integral in the right-hand side of (45), (46), we decompose the real and imaginary parts of each of these integrals as a sum of integrals along consecutive intervals of length π where the integrand has constant sign, and apply the alternating series test to conclude that the complex valued functions

$$\int_{R_0}^x \frac{e^{-iu}}{u} du, \quad \int_{R_0}^x \frac{e^{iu}}{u} du$$

satisfy property \diamond . Regarding the second integrals in the right-hand side of (45), (46), the fact that G_i is bounded and that $\left| \int_{R_0}^x \frac{du}{u^2} \right| = \left| \frac{1}{R_0} - \frac{1}{x} \right|$ imply that the second integrals in the right-hand side of (45), (46) also satisfy property \diamond . Thus we conclude that the functions $B_1(z), B_2(z)$ satisfy property \diamond .

We next study the modulus of the third integrals on the right-hand sides of (43) and (44). Using again that F_i vanishes at ∞ for $i = 1, 2$, we find $C_i > 0$ depending only on F_i such that $|F_i(z)| \leq C_i |z|^{-1}$ whenever $|z| \geq R'$. Hence,

$$\begin{aligned} \left| \int_0^y e^v F_1(x + iv) dv \right| &\leq \frac{C_1}{R'} \int_0^{|y|} e^v dv = \frac{C_1}{R'} (e^{|y|} - 1), \\ \left| \int_0^y e^{-v} F_2(x + iv) dv \right| &\leq \frac{C_2}{R'} (1 - e^{-|y|}), \end{aligned}$$

which finishes the proof of Assertion 7.3. \square

William H. Meeks, III at profmeeks@gmail.com

Mathematics Department, University of Massachusetts, Amherst, MA 01003

Joaquín Pérez at jperez@ugr.es

Department of Geometry and Topology and Institute of Mathematics (IEMath-GR),
University of Granada, 18071 Granada, Spain

References

- [1] J. Bernstein and C. Breiner. Conformal structure of minimal surfaces with finite topology. *Comm. Math. Helv.*, 86(2):353–381, 2011. MR2775132, Zbl 1213.53011.
- [2] J. Bernstein and C. Breiner. Helicoid-like minimal disks and uniqueness. *J. Reine Angew. Math.*, 655:129–146, 2011. MR2806108, Zbl 1225.53008.

- [3] T. H. Colding and W. P. Minicozzi II. An excursion into geometric analysis. In *Surveys of Differential Geometry IX - Eigenvalues of Laplacian and other geometric operators*, pages 83–146. International Press, edited by Alexander Grigor'yan and Shing Tung Yau, 2004. MR2195407, Zbl 1076.53001.
- [4] T. H. Colding and W. P. Minicozzi II. The space of embedded minimal surfaces of fixed genus in a 3-manifold I; Estimates off the axis for disks. *Ann. of Math.*, 160:27–68, 2004. MR2119717, Zbl 1070.53031.
- [5] T. H. Colding and W. P. Minicozzi II. The space of embedded minimal surfaces of fixed genus in a 3-manifold II; Multi-valued graphs in disks. *Ann. of Math.*, 160:69–92, 2004. MR2119718, Zbl 1070.53032.
- [6] T. H. Colding and W. P. Minicozzi II. The space of embedded minimal surfaces of fixed genus in a 3-manifold III; Planar domains. *Ann. of Math.*, 160:523–572, 2004. MR2123932, Zbl 1076.53068.
- [7] T. H. Colding and W. P. Minicozzi II. The space of embedded minimal surfaces of fixed genus in a 3-manifold IV; Locally simply-connected. *Ann. of Math.*, 160:573–615, 2004. MR2123933, Zbl 1076.53069.
- [8] T. H. Colding and W. P. Minicozzi II. The Calabi-Yau conjectures for embedded surfaces. *Ann. of Math.*, 167:211–243, 2008. MR2373154, Zbl 1142.53012.
- [9] T. H. Colding and W. P. Minicozzi II. The space of embedded minimal surfaces of fixed genus in a 3-manifold V; Fixed genus. *Ann. of Math.*, 181(1):1–153, 2015. MR3272923, Zbl 06383661.
- [10] P. Collin. Topologie et courbure des surfaces minimales de \mathbb{R}^3 . *Ann. of Math. (2)*, 145–1:1–31, 1997. MR1432035, Zbl 886.53008.
- [11] L. Hauswirth, J. Pérez, and P. Romon. Embedded minimal ends of finite type. *Transactions of the AMS*, 353:1335–1370, 2001. MR1806738, Zbl 0986.53005.
- [12] W. H. Meeks III and J. Pérez. Finite type annular ends for harmonic functions. Preprint at <http://arXiv.org/abs/0909.1963>.
- [13] W. H. Meeks III and J. Pérez. The classical theory of minimal surfaces. *Bulletin of the AMS*, 48:325–407, 2011. MR2801776, Zbl 1232.53003.
- [14] W. H. Meeks III and J. Pérez. *A survey on classical minimal surface theory*, volume 60 of *University Lecture Series*. AMS, 2012. ISBN: 978-0-8218-6912-3; MR3012474, Zbl 1262.53002.
- [15] W. H. Meeks III, J. Pérez, and A. Ros. The embedded Calabi-Yau conjectures for finite genus. Work in progress.
- [16] W. H. Meeks III, J. Pérez, and A. Ros. The local picture theorem on the scale of topology. Preprint at <http://arxiv.org/abs/1505.06761>.

- [17] W. H. Meeks III, J. Pérez, and A. Ros. Local removable singularity theorems for minimal laminations. To appear in *J. Differential Geom.* Preprint at <http://arxiv.org/abs/1308.6439>.
- [18] W. H. Meeks III, J. Pérez, and A. Ros. Structure theorems for singular minimal laminations. Preprint available at <http://wdb.ugr.es/local/jperez/publications-by-joaquin-perez/>.
- [19] W. H. Meeks III and H. Rosenberg. The uniqueness of the helicoid. *Ann. of Math.*, 161:723–754, 2005. MR2153399, Zbl 1102.53005.
- [20] R. Osserman. Global properties of minimal surfaces in E^3 and E^n . *Ann. of Math.*, 80(2):340–364, 1964. MR0179701, Zbl 0134.38502.
- [21] H. Rosenberg. Minimal surfaces of finite type. *Bull. Soc. Math. France*, 123:351–354, 1995. MR1373739, Zbl 0848.53004.